

Review

Research Progress on Risk Prevention and Control Technology for Lithium-Ion Battery Energy Storage Power Stations: A Review

Weihang Pan 

School of Electrical Engineering and Automation, Henan Polytechnic University, Jiaozuo 454003, China; 312204040421@home.hpu.edu.cn

Abstract

Amidst the background of accelerated global energy transition, the safety risk of lithium-ion battery energy storage systems, especially the fire hazard, has become a key bottleneck hindering their large-scale application, and there is an urgent need to build a systematic prevention and control program. This paper focuses on the fire characteristics and thermal runaway mechanism of lithium-ion battery energy storage power stations, analyzing the current situation of their risk prevention and control technology across the dimensions of monitoring and early warning technology, thermal management technology, and fire protection technology, and comparing and analyzing the characteristics of each technology from multiple angles. Building on this analysis, this paper summarizes the limitations of the existing technologies and puts forward prospective development paths, including the development of multi-parameter coupled monitoring and warning technology, integrated and intelligent thermal management technology, clean and efficient extinguishing agents, and dynamic fire suppression strategies, aiming to provide solid theoretical support and technical guidance for the precise risk prevention and control of lithium-ion battery storage power stations.



Academic Editor: King Jet Tseng

Received: 3 July 2025

Revised: 30 July 2025

Accepted: 4 August 2025

Published: 6 August 2025

Citation: Pan, W. Research Progress on Risk Prevention and Control Technology for Lithium-Ion Battery Energy Storage Power Stations: A Review. *Batteries* **2025**, *11*, 301. <https://doi.org/10.3390/batteries11080301>

Copyright: © 2025 by the author. Licensee MDPI, Basel, Switzerland. This article is an open access article distributed under the terms and conditions of the Creative Commons Attribution (CC BY) license (<https://creativecommons.org/licenses/by/4.0/>).

1. Introduction

With the acceleration of the global energy transition, the scale of renewable energy is constantly expanding. As an important support for ensuring the stable supply and efficient utilization of energy, the significance of energy storage technology is becoming increasingly prominent. According to incomplete statistics from the CNESA DataLink Global energy storage database [1], by the end of 2024, China's cumulative installed capacity of power energy storage exceeded the gigawatt mark for the first time, reaching 137.9 GW. Among them, the installed capacity of new energy storage surpassed that of pumped storage for the first time. With an installed capacity of 78.3 GW/184.2 GWh, it achieved significant growth in power and energy scale, with year-on-year growth rates as high as 126.5% and 147.5%. Among various new energy storage technologies, lithium battery energy storage power stations are widely used in multiple fields, such as peak shaving, frequency regulation, backup power supply, and grid connection of renewable energy in the power system, thanks to their advantages of short construction period, flexible deployment, and

fast response speed [2–4]. As of the first half of 2024, in the proportion of the new energy storage installations, lithium-ion battery (LIB) energy storage installation projects accounted for approximately 97%, becoming the mainstream energy storage technology at present and holding an absolute advantage.

However, despite the remarkable development achievements of lithium battery energy storage technology, its wide application has also brought many challenges. In recent years, safety issues such as thermal runaway of lithium batteries, fires, and explosions in energy storage power stations have occurred frequently, posing a huge threat to life and property and sounding the alarm for the sustainable development of the energy storage industry. Behind these accidents, there are many deficiencies in the risk prevention and control of current lithium battery energy storage technology. For instance, the monitoring and early warning technology for lithium batteries is not perfect, the fire extinguishing agents are not targeted enough, and the battery early warning system cannot be effectively linked with the fire protection system. These problems not only seriously threaten personnel safety but also restrict the large-scale application and industrialization of lithium battery energy storage.

Against this backdrop, a large number of scholars and researchers have conducted in-depth studies on safety risk prevention and control technologies for lithium battery energy storage and have made some progress. This paper takes lithium battery energy storage power stations as the research object. It conducts a comprehensive review of their complex fire characteristics and thermal runaway mechanism, as well as the monitoring and early warning technology, thermal management technology, and fire extinguishing technology of the energy storage power stations. Through an in-depth analysis of the existing technologies, the aim of this study is to explore the best technical risk prevention and control solutions, providing a solid guarantee for the safe operation of lithium battery energy storage power stations in the future.

2. Fire Characteristics and Mechanism of Thermal Runaway (TR) of LIB Energy Storage Power Station

2.1. Fire Characteristics of LIB Energy Storage Power Station

The types of fires caused by lithium-ion battery combustion are complex. As shown in Table 1, fires can be classified into six categories based on the type of combustible materials and combustion characteristics. The combustion of the separator material and the electrodes of LIBs conforms to the characteristics of Class A fires; the combustion of the electrolyte belongs to Class B fires; the combustion of flammable gases produced during the thermal runaway (TR) process of the battery belongs to Class C fires; while the combustion of the battery itself and the electrical equipment inside the battery compartment belongs to Class E fires [5–8]. Therefore, when a fire breaks out in a lithium battery energy storage power station, the evolution of the disaster situation presents multi-dimensional and complex characteristics. Specifically, the rapid spread of the fire, the generation and release of a large amount of toxic gases, and the high difficulty in the firefighting process are the key elements constituting its fire risk, as shown in Figure 1.

2.1.1. The Rapid Spread of the Fire

LIB energy storage power stations have the characteristic of a highly dense battery layout. When a single battery experiences TR due to factors such as heating, mechanical damage, or electrical faults, it will release a large amount of heat energy and flammable gases. TR batteries, as heat sources, cause the temperature of the adjacent batteries to rise rapidly through the heat conduction mechanism. Meanwhile, the thermal radiation effect can also cause the temperature of the outer casing and the internal active substances of the surrounding batteries to rise. When the temperature reaches the TR threshold of

the adjacent battery, a chain TR reaction is triggered. This chain reaction spreads at an extremely fast speed within the battery module, causing the fire to break out in multiple points within an extremely short period of time. The entire energy storage compartment and even adjacent compartments may fall into a state of full-scale combustion within minutes, forming a three-dimensional and multi-area fire spread pattern, which greatly compresses the time window for early fire warning and emergency response.

Table 1. The basic types of fire.

Type of Fire	Type of Combustible Substance	Combustion Characteristics
Class A fire	Solid substances, which usually have the properties of organic substances	Produce scorching embers when burned
Class B fire	Liquid or solid substances that can be melted	The flame is relatively high, the burning speed is fast, and it is prone to boiling over and splashing.
Class C fire	Gaseous combustible materials	The flame is blue or purple, burns quickly, leaves no residue, and is prone to explosion
Class D fire	Metallic combustibles	Produce strong light and a lot of calories; may trigger strong reactions; the traditional fire extinguishing agent is difficult to extinguish.
Class E fire	Live equipment or electrical circuits	Produce high temperature and toxic gas, accompanied by arc and electric spark
Class F fire	Cooking oils or fats	The flame temperature is high, and it is prone to boiling over and splashing

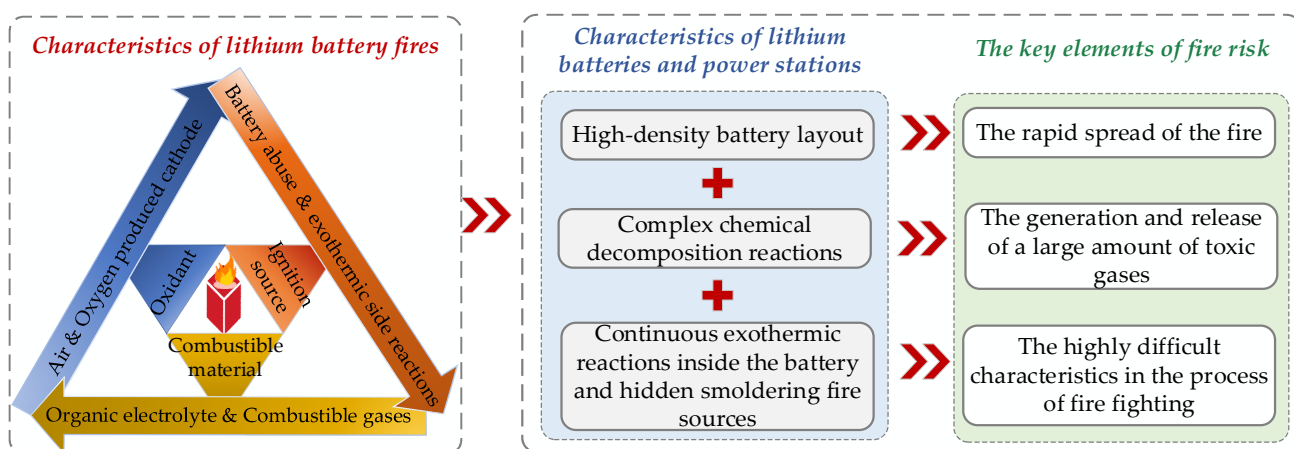


Figure 1. Key elements of fire risk in lithium battery energy storage power stations (adapted with permission from Refs. [8,9]).

2.1.2. The Generation and Release of a Large Amount of Toxic Gases

Before and during the combustion of lithium ions, complex chemical decomposition reactions occur among various components inside the battery. Organic solvents (such as carbonate compounds) in the electrolyte of LIBs undergo thermal decomposition reactions under high temperatures, generating carbon oxides, such as CO and CO₂. The decomposition of fluorine-containing electrolyte salts (such as lithium hexafluorophosphate) generates gases such as HF that are highly corrosive and toxic; under specific conditions, the cathode material may also release oxygen, which further undergoes oxidation reactions with the decomposition products of organic solvents, intensifying the generation of toxic gases. When these toxic gases mix with smoke, they accumulate rapidly in the enclosed or semi-enclosed space of energy storage power stations, and their concentrations can reach levels

harmful to human health in a short period of time. Once personnel are exposed to such an environment with high concentrations of toxic gases, respiratory tract irritation and chemical pneumonia may occur in a short period of time, and even consciousness disorders may arise due to the neurotoxic effects of the gases, greatly increasing the risk of casualties. At the same time, the leakage of toxic gases will also cause pollution in the surrounding atmospheric environment. The diffusion range and the degree of harm depend on the meteorological conditions at that time and the ventilation conditions of the energy storage power station.

2.1.3. The Highly Difficult Characteristics in the Process of Firefighting

Firefighting in lithium battery energy storage power stations faces many technical difficulties. On the one hand, the TR reaction inside the battery is self-sustaining. Even if the external open flame is extinguished, the active substances and electrolyte inside the battery may still continue to undergo exothermic reactions, and it is difficult to completely eliminate the hidden smoldering fire source, which significantly increases the probability of fire reigniting. On the other hand, the battery modules of the energy storage power stations usually have a high degree of sealing and integration, making it difficult for fire extinguishing agents to effectively penetrate into the interior of each battery cell, which limits the performance of their fire extinguishing efficiency. In addition, traditional fire extinguishing methods have certain limitations: Although water-based fire extinguishing systems can quickly lower the ambient temperature, the contact of water with the live components inside the battery may cause short circuit faults and even pose an electric shock hazard. Although dry powder fire extinguishing agents can block the oxygen required for flame combustion, their inhibitory effect on the internal chemical reactions of batteries is limited, and a large amount of dry powder residue may interfere with the later performance evaluation and repair of batteries. Furthermore, the fire scene at the energy storage power stations is often accompanied by high temperatures, toxic gases, and complex electrical environments. Firefighters find it difficult to precisely locate the fire source at close range and carry out effective firefighting operations. These factors together significantly increase the difficulty of extinguishing fires in lithium battery energy storage power stations, prolong the fire duration, and further intensify the fire losses and the severity of the damage.

2.2. Analysis of the TR Mechanism of LIBs

LIBs have become the first choice for energy storage systems due to their high energy density, long cycle life, wide operating temperature range, and no memory effect [10,11]. However, manufacturing defects or improper operation and maintenance may trigger catastrophic accidents. A large number of studies have shown that TR is a common cause of fire and explosion [12–15]. According to the existing reviews, TR causes can be divided into two categories: “internal causes” and “external causes” (Figure 2). Internal causes: impurities mixed in during the production stage can pierce the diaphragm, resulting in direct contact between the positive and negative electrodes; uneven electrode coating or differences in diaphragm thickness cause local impedance anomalies [16,17]; long-term cycling causes lithium dendrites to grow and penetrate the diaphragm, inducing internal short circuits. External causes include three typical scenarios: thermal abuse—high temperature causes thermal shrinkage of the diaphragm; electrical abuse—overcharging induces negative electrode dendrites; and mechanical abuse—external force extrusion or puncture. The above-mentioned internal and external source coupling effects are ultimately attributed to internal short circuits, which in turn trigger a thermal runaway chain reaction.

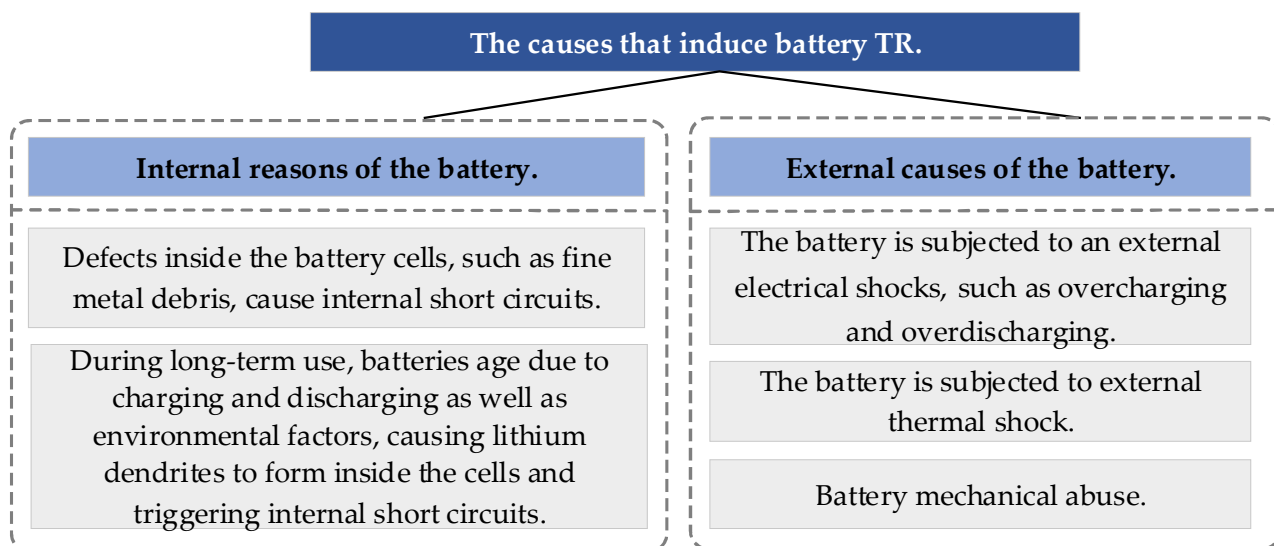


Figure 2. Analysis of the causes inducing battery TR.

TR in LIBs is fundamentally triggered by an internal short circuit, whether the triggering factor is internal performance degradation or external abuse [18,19]. Once a short circuit occurs, local Joule heating causes the battery temperature to rise; if this heat cannot be effectively removed, a positive feedback loop is formed. The first chemical instability occurs at around 69 °C, when the metastable solid electrolyte interface (SEI) layer begins to decompose. Between 90 °C and 120 °C, the organic components of the SEI further decompose into gaseous products, such as CO₂ and C₂H₄, which increase the internal pressure. At the same time, oxygen is released from the delithiation cathode lattice, forming a flammable mixture, which significantly increases the risk of fire or explosion [12,20].

When the temperature exceeds about 150 °C, the polyolefin separator (PE and PP) softens and melts, eliminating the electronic barrier between the anode and cathode. Direct contact between the electrodes establishes a persistent short-circuit path, while the exothermic reaction between the electrolyte and the highly active electrode material further accelerates heat generation. The continued melting of the separator brings more and more electrodes into direct contact, thereby releasing energy at an ever-increasing rate until complete thermal runaway [21]. The resulting temperature excursion may eventually lead to fire or explosion, posing a serious safety hazard to large-scale energy storage devices. Figure 3 schematically summarizes the series of physicochemical events that lead to TR and the subsequent fire spread within a lithium-ion battery energy storage system.

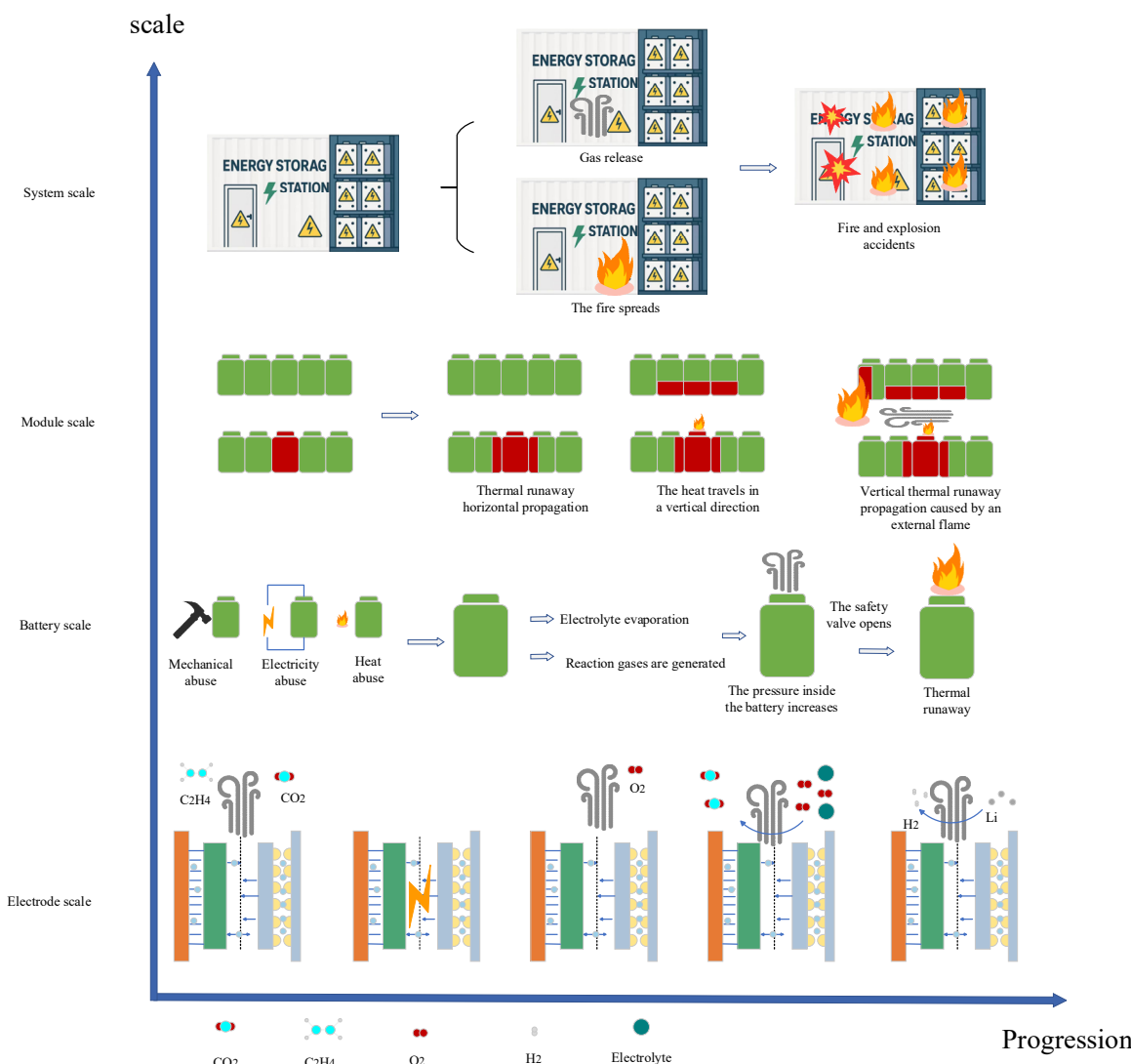


Figure 3. Diagram showing the timeline of TR in LIBs (Reprinted/adapted with permission from Ref. [22]).

It should be noted that although aging is considered as one of the internal causes of thermal runaway (TR), most of the existing literature only provides a qualitative description. Through the horizontal comparison of the gas monitoring results of Zhang et al.'s [23] 243 Ah LFP module experiment, Meng et al.'s [24] 14 Ah LFP experiment, and Wang et al.'s [25] 8.8 kWh module, it can be found that when SOH decreases from 100% to 80%, the TR trigger temperature decreases by 5–9 °C, the CO and H_2 yield increases by 20–35%, and the reburning probability increases from $\leq 30\%$ to $\geq 60\%$. Although these public data are not enough to establish a universal equation, they are enough to show that the degree of aging is significantly positively correlated with safety risks. Therefore, in engineering applications, stricter temperature thresholds, earlier warning triggers, and longer continuous spraying time of fire extinguishing agents should be adopted for battery packs with $\text{SOH} \leq 85\%$ to make up for the lack of quantification of aging risks by existing technologies.

3. Monitoring and Early Warning Technology for LIB Energy Storage Power Stations

Early monitoring and early warning technology for energy storage power stations mainly focuses on the monitoring and early warning of TR of lithium batteries, aiming to issue early warning signals when battery failures occur but power station fires have not

yet taken place [26]. The TR of lithium-ion batteries has specific characteristic temperature patterns. Based on this pattern, the evolution process of TR can be roughly divided into four stages, namely, before TR, in the early stage of TR, during the occurrence period of TR, and in the early stage of fire. As shown in Figure 4, throughout the entire process of TR evolution, multiple characteristic signals will occur at each stage, including electrical signals (such as voltage, current, and resistance), temperature signals, gas signals, smoke signals, and flame signals. In addition, when lithium-ion batteries are combined into energy storage systems, other forms of signals such as wind, sound, vibration, and strain may also occur [27].

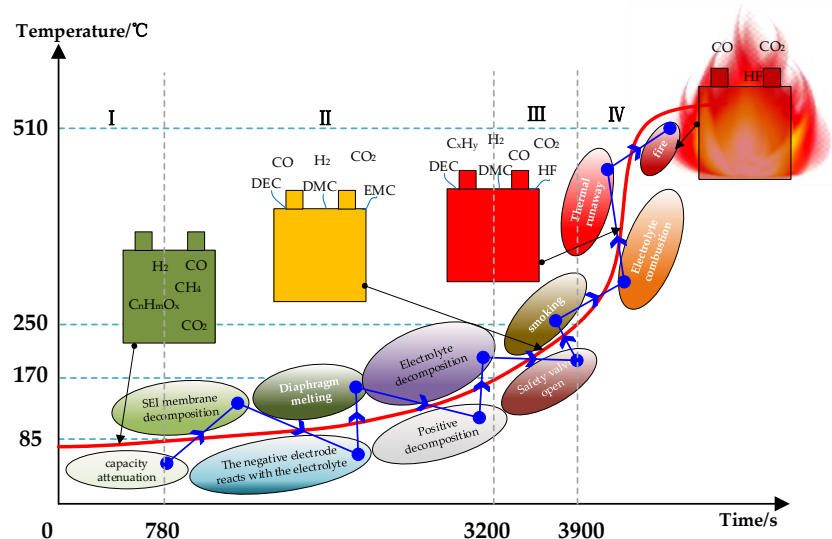


Figure 4. Characteristic phenomena of battery TR (from Ref. [28] open access).

At present, the mainstream methods for discriminating battery TR at home and abroad mainly include the following: (1) The battery management system (BMS) judges the safety status of the battery through data such as the surface temperature, voltage, and current status of the battery [29,30]. (2) By measuring the internal temperature of the battery and other factors, the TR state of the battery during charging and discharging can be reflected [31]. (3) The TR state of the battery can also be determined by the types and concentrations of gases released outside the module by the battery [32]. (4) The state of TR is determined by identifying the characteristic image of the large amount of gas–liquid overflow released after TR [33]. (5) Utilize other characteristic signals such as the sound signal of battery exhaust, internal air pressure, and expansion force to make TR judgments [34]. Table 2 summarizes the current mainstream methods for discriminating battery TRs.

Table 2. The current mainstream methods for discriminating battery TR.

Discrimination Method	Discrimination Basis	Early Warning Effect	References
BMS	Battery surface temperature, voltage, current, etc.	The operation is simple, but the temperature difference between the inside and outside of the battery is large, and the early warning has significant limitations and lag.	[29]
Battery-embedded fiber Bragg sensor	The relationship between the internal charge state and the wavelength of the optical fiber refraction is established.	The early warning is timely and effective, but it is costly and prone to damaging the battery structure.	[35]

Table 2. Cont.

Discrimination Method	Discrimination Basis	Early Warning Effect	References
Impedance phase shift	The phase shift of the battery impedance corresponds to the internal temperature.	The early warning is timely and effective, but it is highly dependent on precision measurement instruments, and the device cost is high.	[36]
Battery dynamic impedance at single frequency point	The relationship between the dynamic impedance of the battery at single frequency point and the internal temperature	The early warning time is 580 s ahead of thermal runaway. It has low cost, simple operation, and does not rely on precision instruments.	[37]
Characteristic gas concentration	H ₂ and CO produced in the early stage of battery thermal runaway.	It can achieve extremely early warning of thermal runaway and has a low installation cost.	[38,39]
Feature sound recognition	The sound of the safety valve and the pressure relief valve opening	It can achieve thermal runaway alarm and fault module location.	[34,40]
Expansion force	Internal lithium-ion battery-embedded sensor; precipitation will result in the thickening of the batteries, producing expansive force.	The early warning is timely and effective, but it is highly dependent on precision measurement instruments, and the device cost is high.	[41]
Smoke concentration and images	Gas-liquid emissions produced by high temperatures and side reactions	The operation is simple, but there is a lag in early warning.	[42]

3.1. TR Discrimination Methods Based on the BMS for Monitoring and Early Warning in LIB Energy Storage Power Stations

BMS is a core component of lithium-ion battery energy storage power stations. Its main functions include battery condition monitoring, charge and discharge management, thermal management, and early safety warning [43]. BMS can monitor parameters such as the surface temperature, voltage, and current of the battery in real time. Through the analysis and processing of these parameters, it can promptly detect abnormal states of the battery [44]. Due to the large scale of the battery, the BMS of the energy storage power station usually adopts a three-tier architecture of the battery management unit (BMU), the battery control unit (BCU), and the battery administration unit (BAU) to achieve efficient management of multiple batteries, as shown in Figure 5. The BMU is responsible for directly monitoring and controlling each individual battery cell, collecting data such as the voltage and temperature of each individual battery cell, and conducting preliminary data processing and analysis to ensure that each battery cell operates within the specified safety range. The BCU receives the data transmitted by the controlled BMU, conducts further processing and analysis, coordinates the work of each BMU, and makes reasonable decisions based on the overall operating status of the battery pack, such as adjusting the charging and discharging strategies. As the core control unit of the entire BMS, the master control BAU is responsible for receiving the data summary of the BCU for global monitoring and management. At the same time, it communicates and coordinates with other systems of the energy storage power station, such as interacting with the energy management system (EMS). According to the operation requirements of the power station,

the charging and discharging power of the battery is reasonably allocated to ensure the safe, stable, and efficient operation of the entire energy storage power station.

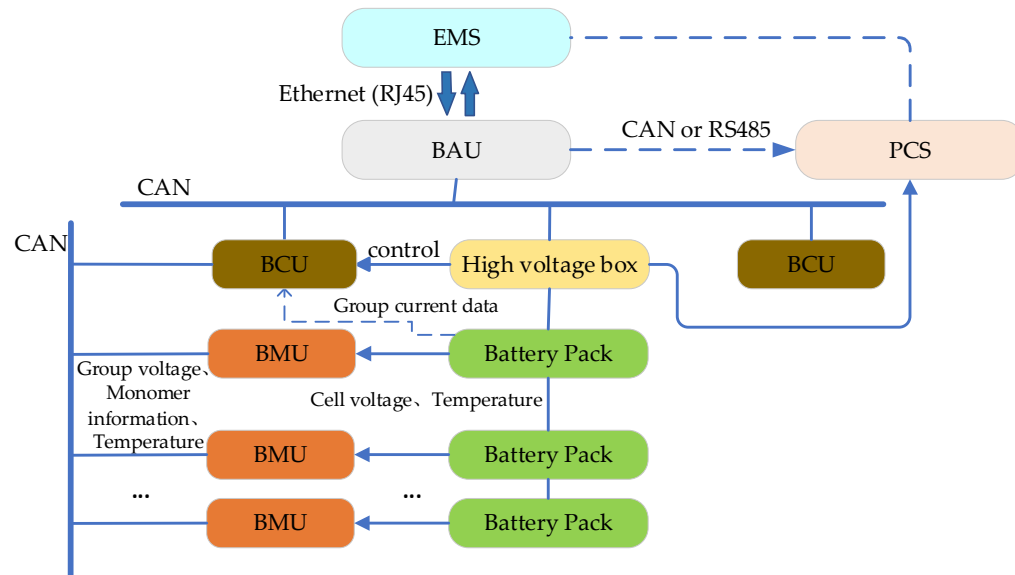


Figure 5. BMS architecture of energy storage power stations.

However, at present, the computing power and storage space of BMS are limited, and it cannot directly and comprehensively perceive the internal situation of lithium batteries. Therefore, it is unable to provide early warnings of safety accidents from the root cause [45]. In view of this, many researchers are committed to deeply integrating big data technology, advanced algorithms, and precise models with BMS, aiming to achieve dynamic monitoring of the state of charge (SOC) and health status (SOH) of batteries, thereby enhancing the refinement level and safety of battery management. Liu et al. [46] proposed a SOC estimation method combining convolutional neural network (CNN) and Long Short-Term Memory Network (LSTM). The CNN module extracts the spatial characteristics among multiple variables such as voltage, current, and temperature, and the LSTM module models the dynamic time relationship of the charging and discharging process, forming an end-to-end CNN–LSTM joint network. Experiments show that the average error of this model in predicting SOC is only 0.65%, which is 4.4% lower than that of the single CNN model. It is reduced by 0.2% compared with the single LSTM model and has good adaptability and stability under different battery working conditions. Wu et al. [47] focused on the modeling of current characteristics in the constant voltage charging stage of batteries. They extracted statistical features such as the slope at the beginning and end points, standard deviation, and mean from the current curve to form a new combination of health features as the input for SOH modeling. Experiments have proved that this feature combination can achieve high-precision SOH estimation in multiple models and has good model adaptability. Fan et al. [48] proposed an SOH estimation method for lithium-ion batteries based on two-stage charging data fusion. This method breaks through the traditional limitations and innovatively integrates the data of the constant voltage charging stage and the relaxation stage, significantly improving the adaptability and practicability of SOH estimation. The test results show that the average absolute error of SOH estimation of this method is 0.66%, and the average determination coefficient reaches 0.97. The accuracy is significantly better than that of the traditional methods. Zheng et al. [49] proposed a residual convolution and transformer network for SOH estimation in the random voltage segment. This method utilizes the features of sparse dimensions in random segments to achieve an accurate SOH estimation of lithium-ion batteries. It integrates

the operating conditions and segment positions through the cross-attention mechanism of residual convolution and the transformer network (R-TNet), thereby realizing SOH estimation within the charging segment. To extend the flexibility of any charging behavior, the elastic network was designed based on the feature transport strategy of ElasticNet to adapt to any charging length. It was verified using 121 batteries with different chemical compositions and cycling conditions. The results show that even for the 50 mV voltage segment, the root mean square error of SOH estimation can reach 1.6%.

3.2. TR Discrimination Methods Based on the Battery Internal Temperature for Monitoring and Early Warning in LIB Energy Storage Power Stations

TR is characterized by an uncontrolled, self-accelerating temperature rise driven by mutually reinforcing exothermic side reactions; it is therefore a strongly non-linear phenomenon rather than a simple thermal excursion. Sun et al. [50] demonstrated that under normal cycling, a pronounced radial thermal gradient exists between the core and the surface of a lithium-ion cell. Consequently, surface-temperature measurements alone are insufficient to identify the onset of TR; core-temperature data are required for reliable detection.

Battery-state monitoring at the cell interior is typically realized through embedded sensors that register temperature, pressure, or impedance. Bragg grating fiber-optic sensors are presently the most advanced technique for this purpose. Mei et al. [51] fabricated a miniature multi-parameter fiber probe that can be inserted into commercial cells and continuously tracks both core temperature and internal pressure throughout TR propagation. Fernandes et al. [52] employed a similar fiber Bragg grating (FBG) to monitor dynamic changes in refractive index caused by local temperature or pressure variations; these changes are transduced into measurable wavelength shifts, enabling real-time, multi-point diagnostics. The principal advantages of FBG sensors include micro-scale footprint, immunity to electromagnetic noise, remote interrogation capability, and simultaneous multi-parameter sensing. Their widespread adoption is nevertheless hindered by high unit cost and stringent manufacturing tolerances, which currently limit large-scale commercial deployment. Despite these barriers, FBG-based diagnostics continue to attract significant research and industrial interest.

As a complementary, non-intrusive alternative, electrochemical impedance spectroscopy (EIS) has been exploited to infer core temperature from surface measurements. Leng et al. [53] established that the imaginary component of impedance within 0.1 Hz– 5×10^4 Hz exhibits a monotonic and stable correlation with internal temperature. Building on this finding, Lei et al. [54] developed an algorithm that combines impedance magnitude and phase data at selected frequencies to estimate core temperature with high fidelity, offering a cost-effective solution for TR early warning when embedded sensors are impractical.

3.3. TR Discrimination Methods Based on the Gas Signal for Monitoring and Early Warning in LIB Energy Storage Power Stations

Table 3 summarizes the principal gaseous species released during lithium-ion-battery TR. Because these products are generated prior to visible venting or ignition, their detection offers a promising route for non-intrusive early warning.

Wang et al. [1] quantitatively sampled the vent gases and observed that the CO concentration exhibited the sharpest increase immediately before the safety valve burst, while the cell surface temperature remained below 100 °C. They therefore proposed a dual-parameter criterion—CO concentration plus surface temperature—for TR prediction. Subsequent work has refined this strategy by assigning specific gases to distinct alert levels. Hydrogen, CO, and CO₂ show the earliest and most pronounced concentration rises and

constitute a first-level alarm; HCl and HF, which appear later, serve as a second-level confirmation when the primary indicators are ambiguous.

Complementary diagnostic approaches have also been explored. Kim et al. [55] employed *in situ* Raman spectroscopy to monitor the headspace of aged supercapacitors, verifying that H₂ and CO dominate the off-gas and that Raman sensing can be performed non-destructively. Jin et al. [56] demonstrated that micrometre-scale lithium dendrite formation can be inferred from minute increases in H₂ concentration, underscoring the sensitivity of hydrogen-based detection. Zheng [57] constructed a single-cell TR test bench for 8.8 kWh Lithium Iron Phosphate (LiFePO₄) modules and showed that H₂ was the first detectable species—preceding smoke by 639 s and visible fire by 769 s—thereby confirming its value as an advance indicator.

At the module level, Wang et al. [58] integrated visible-light cameras, infrared imaging, and multi-species gas sensors in a full-scale energy-storage chamber. Their results revealed distinct gas-evolution profiles corresponding to successive TR stages in both hard-case and pouch LiFePO₄ modules. Similarly, Fernandes et al. [52] subjected commercial LEP cells to overcharge abuse and used a high-resolution gas-analysis platform to identify and quantify the evolved species, laying the groundwork for a quantitative TR early-warning algorithm based on gas fingerprints.

Collectively, these studies establish that real-time gas sensing—particularly of H₂ and CO—can provide tens to hundreds of seconds of advance notice before conventional thermal or smoke alarms, offering a practical and scalable complement to the existing battery-management systems.

Table 3. The main side reactions inside the battery [59–62].

Chemical Reaction Process	Chemical Reaction Equation	The Main Types of Gas Produced
Decomposition of SEI film	(CH ₂ OCO ₂ Li) ₂ → CO ₂ ↑ + C ₂ H ₄ ↑ + Li ₂ CO ₃	CO ₂ ; C ₂ H ₄
The negative electrode reacts with the electrolyte.	EC + Li ⁺ + e [−] → Li ₂ CO ₃ + C ₂ H ₄ ↑ DEC + Li ⁺ → LiOCO ₂ C ₂ H ₅ + C ₂ H ₅ OC ₂ H ₅ ↑ EC → CO↑ + CH ₄ + H ₂ ↑	C ₂ H ₄ ; H ₂ ; C ₂ H ₅ OC ₂ H ₅ ; CO
Decomposition of cathode materials (such as LiCoO ₂)	LiCoO ₂ → Li _{1-x} CoO ₂ + xLi + 1/2O ₂ ↑ C + O ₂ → CO ₂ ↑	O ₂ ; CO ₂
LiPF ₆ in the electrolyte decomposes.	LiPF ₆ → LiF + PF ₅	
The product of DEC, C ₂ H ₅ OCOOPF ₄ , further decomposes. Meanwhile, C ₂ H ₅ OCOOPF ₄ also reacts with HF.	C ₂ H ₅ OCOOPF ₄ → CO ₂ ↑ + PF ₅ ↑ + C ₂ H ₅ F↑ C ₂ H ₅ OCOOPF ₄ + HF → POF ₃ ↑ + C ₂ H ₆ ↑ + CO ₂ ↑ + H ₂ O	CO ₂ ; PF ₅ ; C ₂ H ₅ F; POF ₃ ; C ₂ H ₆
The cathode material (such as graphite) reacts with the electrolyte (such as ethylene carbonate (EC); the chemical molecular formula is C ₃ H ₄ O ₃) in the presence of O ₂	EC + O ₂ → CO ₂ ↑ + H ₂ O	CO ₂

A large number of studies have shown that there is no absolute sequence of chemical side reactions inside batteries, and multiple reactions may occur simultaneously [63]. Moreover, the content of H₂ and CO in the air itself is relatively low. Therefore, H₂ and CO can be used as the basis for early determination of thermal runaway in lithium batteries, providing key clues for early warning [64].

3.4. TR Discrimination Methods Based on the Sound Signals for Monitoring and Early Warning in LIB Energy Storage Power Stations

The lithium iron phosphate battery used for energy storage is a square hard aluminum shell battery, and a safety valve is installed on the top of the battery shell. Due to the large amount of gas produced after battery failure, the internal pressure of the battery

increases [65]. The main function of the safety valve is to release the internal pressure of the battery in time to prevent the internal pressure from continuously increasing and causing an explosion. When the safety valve opens, it produces a distinct sound. There is a certain pattern between different frequency components of this characteristic sound signal. In addition, the acoustic signal has excellent propagation characteristics and is not easily blocked by the module housing and battery rack [66]. Therefore, the characteristic sound signal of this safety valve opening can be used as a parameter for early safety warning.

The monitoring and early warning technology for sound signals of energy storage batteries has undergone significant research and development during the following periods. In 2019, Jin et al. [67] proposed to analyze the time-domain and frequency-domain spectra of the sound of the safety valve opening and the noise inside the battery compartment and study the characteristic laws of the sound signal of the safety valve opening and designed a system for sound signal acquisition, as shown in Figure 6a. In 2020, Li et al. [68] collected various working data of battery energy storage systems, including acoustic signals, comprehensively predicted the operation trend of the energy storage systems, and set the early warning level for fire safety of the battery energy storage systems. The accuracy rate reached 99.7%, as shown in Figure 6b. In 2021, Su et al. [34] proposed to use spectral subtraction for denoising preprocessing in response to the diverse types of interference noise inside the energy storage cabin and constructed a recognition classifier using the XGBoost model to identify the MFCC coefficients of the extracted acoustic signals. Based on the above achievements, Lyu et al. [40] proposed a battery fault alarm and location method based on acoustic signals. By installing only four acoustic sensors in the corner of the energy storage compartment, the exhaust sound signal can be captured when the battery malfunctions, and the spatial position of the battery can be calculated, as shown in Figure 6c. In 2022, the multi-parameter early warning system for thermal runaway of energy storage power stations developed by Jiangsu Electric Power Research Institute utilized technologies such as the recognition of the sound characteristics of battery safety valves opening. Through a deep neural network model, it achieved a highly sensitive identification and early warning of battery fire hazards. The early warning signal was issued 12 min earlier than battery thermal runaway and over 200 s earlier than the traditional single hydrogen early warning. The identification accuracy rate exceeds 97.4%. In 2023, Su et al. [69] started from the thermal runaway experiments of battery cells and modules, verified the effectiveness and sensitivity of sound signal early warning, and proposed an early warning method for thermal runaway based on the recognition of sound signals from safety valves in energy storage compartments, as well as a fault battery location method based on sound source location. Xie et al. [70] adopted a multimodal lithium battery voiceprint recognition device to collect the sound characteristics emitted during the operation of lithium batteries, extracted the voiceprint feature parameters, calculated the power spectrum of the voiceprint signal, and designed a lithium battery energy storage early warning system in combination with edge computing technology. In 2024, Suzhou Times Huajing New Energy Co., Ltd. (A Chinese company) provided an early safety warning method and system for lithium battery energy storage devices based on acoustic signals, which included steps such as determining the coordinates of the battery safety valve, arranging the acoustic signal collection device, and constructing an environmental sound feature set. After the processing of the noise reduction of the acoustic signal collection results, an early safety warning was achieved. In 2025, the early safety warning system for electrochemical energy storage developed by Xihe Intelligent (A Chinese company) was successfully applied. The system consists of three parts: characteristic sound warning, characteristic gas warning, and characteristic image warning. Through the system monitoring of the monitoring platform, the warning can be advanced by 15 min.

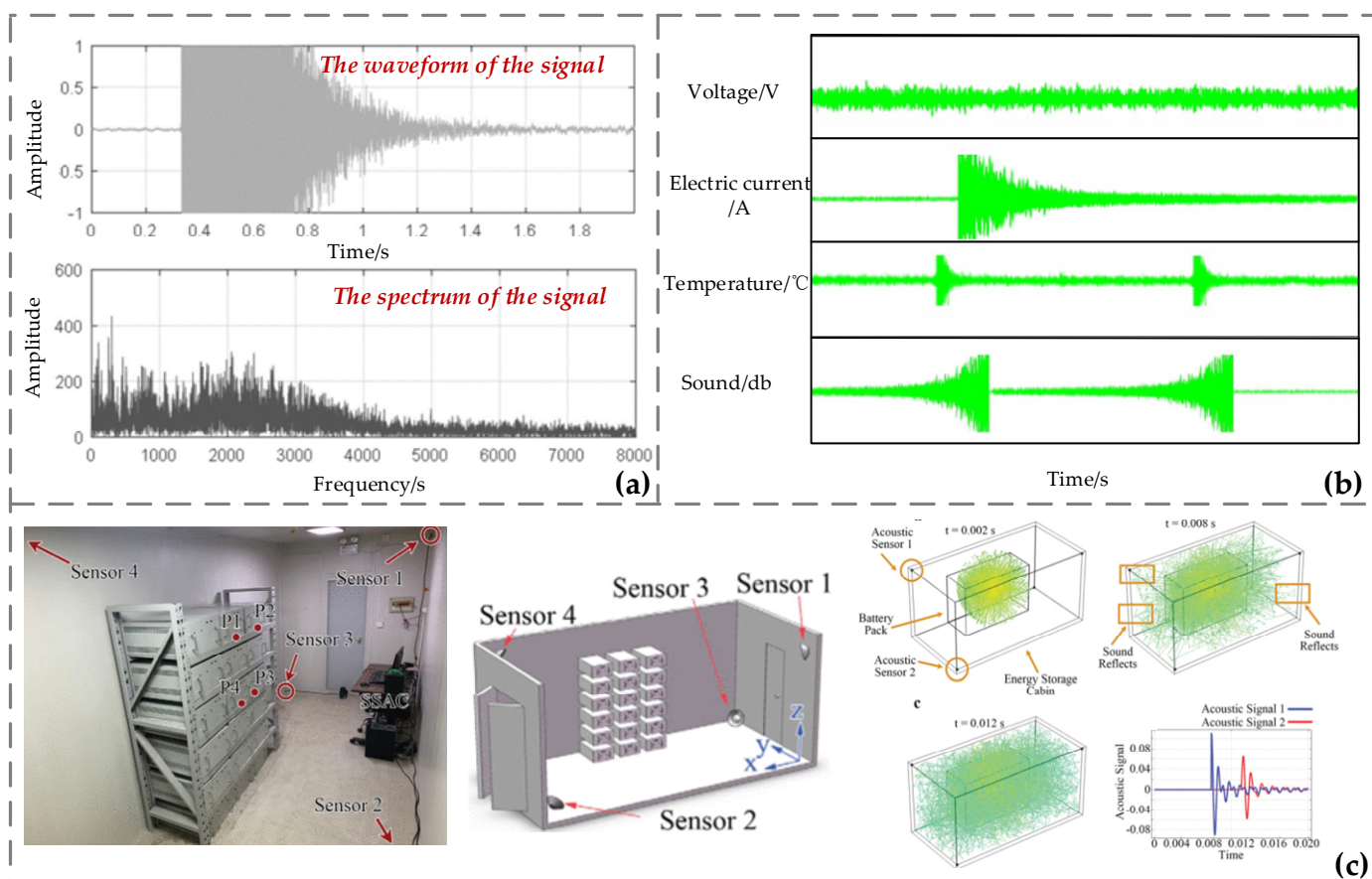


Figure 6. Research on monitoring and early warning technology based on sound signals. (a) Time-domain and frequency-domain spectra of safety valve opening sounds (from Ref. [67] open access). (b) Output results of early warning parameters for batteries (from Ref. [68] open access). (c) The acoustic signal scattering model in the energy storage cabin and the waveforms received by acoustic sensors at different positions (Reprinted with permission from Ref. [40]).

3.5. TR Discrimination Methods Based on the Expansion Force Signals for Monitoring and Early Warning in LIB Energy Storage Power Stations

Battery expansion force refers to the mechanical stress generated during the charging and discharging process of a battery due to volume changes caused by internal chemical reactions. This phenomenon is particularly common in lithium-ion batteries, mainly due to the following reasons: (1) The process of lithium intercalation and deintercalation of active substances: The lithium evolution phenomenon causes metallic lithium to deposit on the surface of the graphite anode, which in turn leads to abnormal and sharp increases in the thickness and expansion force of the battery [71]. (2) Electrolyte decomposition: Side reactions produce gas, increasing internal pressure. (3) Temperature changes: High temperatures accelerate chemical reactions and intensify expansion. (4) Aging effect: After the battery is recycled, the structure of the electrode material deteriorates, and the expansion force increases. Excessive expansion of the battery can lead to deformation of the battery casing, internal short circuits, and even thermal runaway, seriously affecting the safety and lifespan of the battery. Li et al. [72] conducted experimental research on lithium iron phosphate battery cells and modules under thermal abuse mode, revealing the temporal relationship among expansion force, voltage, and temperature, and proposed an early safety warning method based on expansion force, successfully achieving a warning approximately 375 s before battery thermal runaway. It is indicated that the expansion

force signal provides an early warning of battery faults more effectively than the voltage and temperature signals.

At present, scholars at home and abroad have conducted extensive research on the monitoring technology of the expansion force of lithium-ion batteries, as shown in Figure 7. It can mainly be divided into two categories: (1) Direct measurement: By using external or embedded mechanical sensors to measure the expansion force in real time, the changes in the expansion force of the battery can be intuitively reflected, including both built-in sensors and external sensors. (2) Indirect measurement: By using digital imaging technologies, electrochemical impedance spectroscopy, mechanical detection, and other types of sensors, the expansion force is calculated based on certain correlation models or algorithms. Table 4 summarizes the advantages and disadvantages of the above-mentioned several types of expansion force monitoring technologies.

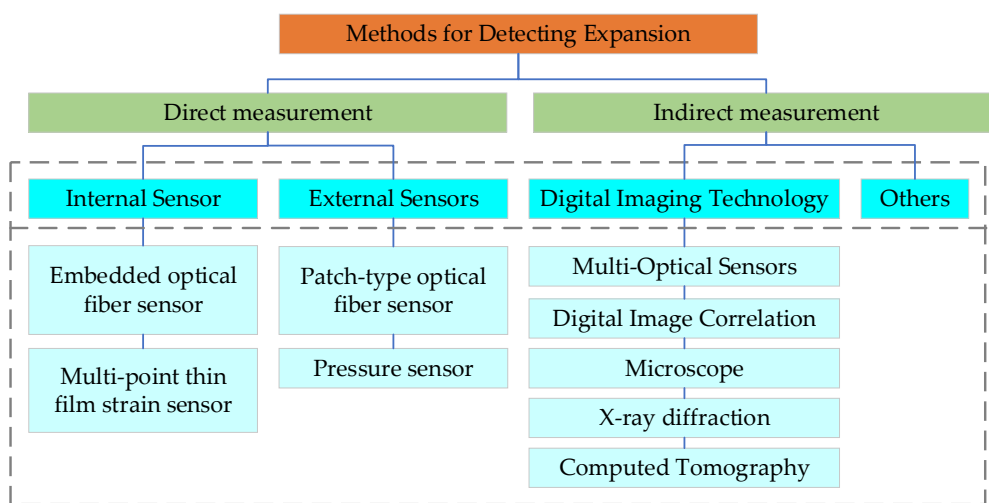


Figure 7. Classification of battery expansion force monitoring methods.

Table 4. The current mainstream methods for monitoring battery expansion force.

Expansion Force Monitoring Method	Advantages	Disadvantages
External pressure patch sensor; patch-type optical fiber sensor	Stick on the outer surface of the battery; will not cause damage to the integrity of the battery.	Not precise enough; low sensitivity. It is difficult to understand the internal chemical changes.
Embedded pressure sensor	It is not affected by factors such as battery case shielding and external temperature and is more accurate and sensitive.	Subject to strong electromagnetic interference and corrosive environmental interference. The operation is complex. Expensive price
Based on digital imaging technology; electrochemical impedance spectroscopy; mechanical detection; and other types of sensors	With the help of other instruments, the integrity of the battery will not be damaged.	With the help of other instruments, the integrity of the battery will not be damaged.

In terms of direct measurement, Figueroa-Santos et al. [73] detected the overall expansion force of the battery by using a fixture to fix the battery and fixing the pressure sensor between the movable plate and the aluminum end plate of the fixture. Cai et al. [74] fixed the pressure sensor at the four corners of the steel plate to detect the expansion characteristics of the battery more evenly and accurately. By jointly detecting the internal short circuit phenomenon of the battery through pressure detection and voltage detection, the accuracy of fault detection was improved. Aufschläger et al. [75] developed a new type of mechanical compression test bench. Three pressure sensors were attached to the

aluminum plate fixture, and the base plate was made of polished granite to achieve a more uniform pressure distribution. This device can be used to measure the expansion changes within the battery when the pressure is between 0.075 and 1.75 MPa. Hemmerling et al. [76] designed an in situ detection system for gas pressure. By inserting a temperature sensor into the cavity at the center of a cylindrical battery coil and pressing the pressure sensor onto a sealed cover plate to ensure uniform contact with the gas pressure generated during the battery cycle, the difference between the internal gas pressure of the battery and the ambient pressure was detected through the cover plate and the hole at the center of the battery. This method solved the problem of the fixture device not being suitable for cylindrical batteries. Pan et al. [77] have developed a novel in situ monitoring technology based on integrated ionized sensing technology. By using the electrolyte and materials of lithium-ion batteries themselves to construct the sensing interface, it can precisely monitor the expansion force without additional packaging, respond to changes at the pack level, and operate stably for over one month. It can capture the irreversible deposition of lithium dendrites, opening up a new path for the design of smart batteries. In terms of indirect measurement, Zhao et al. [78] proposed the use of a multi-dimensional laser scanning method to detect the non-uniformity and defects of lithium battery expansion. Through this method, the relationship between the non-uniform volume expansion observed in fresh batteries and the abnormal deposits on the electrodes after aging was discussed. This method indicates that computed tomography (CT) can verify battery design and evaluate manufacturing quality and also proves that the detection of local non-uniformity of batteries can be used as a non-destructive battery quality inspection tool. Yu et al. [79] monitored the spacing changes of crystal electrode materials in situ through X-ray diffraction (XRD) to determine the lithiation degree of lithium batteries and thereby evaluate the expansion characteristics of the batteries. Ozdogru et al. [80] established a real-time detection system by using digital image correlation technology. Through DIC measurement, it provided the temporal and spatial resolution of chemical and mechanical deformation in solid electrolytes during symmetrical battery cycles. It can measure not only planar deformation but also out-of-plane deformation. Wang et al. [81] proposed an improved 3D-DIC method considering mechanical constraints and applied it to the measurement of the out-of-plane displacement field of thin films. This method retains the advantages of traditional methods, such as easy implementation, rapid convergence, and high efficiency, and improves the disadvantages of traditional methods, such as the lack of spatial continuity and the loss of boundary displacement information.

3.6. TR Discrimination Methods Based on the Smoke Signals for Monitoring and Early Warning in LIB Energy Storage Power Stations

When the safety valve of the battery opens, as the reaction of the electrolyte inside the battery continues, the vaporized electrolyte is continuously sprayed out to the outside of the battery through the safety valve, thereby forming smoke. Electrolyte, as a key component of lithium-ion batteries, is usually composed of non-aqueous organic solvents and lithium salts. In energy storage power stations, traditional smoke detection mainly relies on smoke alarms. However, this approach has a relatively high false alarm rate and missed alarm rate. Moreover, if the control of the alarm's sensitivity is not precise enough, it is very likely to cause unnecessary waste of fire protection resources.

Based on this, scholars at home and abroad are dedicated to conducting relevant research on thermal runaway alarms from the perspectives of smoke image recognition and the properties of gases in the air (such as electrical conductivity, scattering characteristics, etc.), aiming to enhance the accuracy and reliability of the alarm and optimize the safety monitoring and early warning system of energy storage power stations. Tang et al. [82] proposed an algorithm called You Only Look Once, version 3 (YOLOv3), which can realize

the rapid and accurate identification of the vaporized electrolyte in the energy storage cabin, effectively reduce the model volume, improve the model prediction speed, and reduce the hardware cost of model deployment. The average accuracy of the model test on the GTX 1650 graphics card (SOYO GTX 1650; The manufacturer is named SOYO and is located in Shenzhen, China) is 83.65%, and the average prediction rate is 65 frames per second, which meets the requirements of rapid and accurate real-time detection of the vaporized electrolyte in the lithium-ion battery energy storage chamber and shows good results in practical applications. Shi et al. [83] developed an aerosol identification method based on the scattering asymmetry ratio and experimentally measured the scattering asymmetry ratios of different types of aerosols. The results show that under the action of the 870 nm LED light source and when the forward and backward scattering angles are 45° and 135°, respectively, the AR change rate of the electrolyte fire smoke is significantly higher than that of other types of aerosols. Therefore, this aerosol identification method based on the scattering asymmetry ratio can be used for the detection of electrolyte fire smoke. Lin et al. [84] have developed an artificial intelligence detection system based on image recognition and big data analysis for white fog, smoke, and flames in lithium-ion battery storage areas. This system can effectively warn of white fog within 1 min, which is 5 to 10 min faster than the response time of ceiling-mounted and smoke-sensing fire detectors.

4. Thermal Management Technology for Energy Storage Power Stations

During the charging and discharging process of batteries, problems such as heat accumulation and uneven temperature distribution are inevitable. These issues can easily lead to the occurrence of battery thermal runaway, affecting battery performance and lifespan. In more serious cases, they may even cause safety accidents, such as fires and explosions. The thermal management technology of energy storage power stations can ensure that batteries operate within the optimal temperature range, extend battery life while preventing thermal spread, and guarantee the safe, efficient, and long-life operation of the energy storage system. At present, the mainstream thermal management technologies for energy storage power stations mainly include air cooling technology, liquid cooling technology, and phase-change cooling technology.

4.1. Air-Cooling Technology

Air cooling technology uses air as the cooling medium and utilizes the air convection generated by fans or natural winds to carry away heat, thereby achieving the control of battery temperature. It is divided into active air cooling and passive air cooling. Active air cooling is the process of cooling and reducing the temperature of batteries through mechanical means such as fans. Passive air cooling relies on temperature differences, concentration differences, etc. to make the air circulate naturally for heat dissipation. The structure of the air-cooling system for energy storage power stations is shown in Figure 8. Due to its simple structural design, low cost, light weight, and ease of maintenance and management, the air-cooling system is widely used in the thermal management of energy storage battery packs [85].

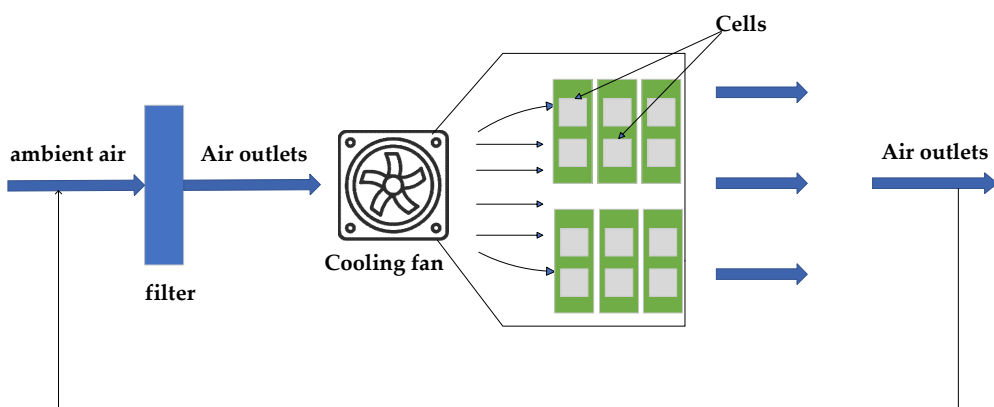


Figure 8. Structural diagram of the air-cooling system for energy storage power stations.

In air-cooled systems, researchers typically enhance the convective heat transfer effect of battery packs by optimizing pipeline design, altering battery spacing, and changing battery sizes, while maintaining the uniformity of battery temperature distribution [86]. Chen et al. [87] improved the cooling efficiency of the air-cooling system by optimizing the system flow channel design. They conducted research on different layout schemes of air inlets and outlets, introduced the CFD method to calculate the flow field and temperature field of the battery thermal management system (BTMS), and concluded that the positions of the inlet area and the outlet area could significantly affect the cooling efficiency of the air-cooling system. Experiments and numerical simulations show that when both the inlet area and the outlet area are located in the center of the air duct, the air-cooling system can achieve more efficient cooling. Xie et al. [88] studied the influences of air intake angle, air outlet angle, and the distance width of battery cells on heat dissipation performance through experiments and simulations. Orthogonal experimental tables were constructed for these three factors. The parameters were adjusted and optimized through the methods of single-factor analysis and orthogonal experiments. The results show that when the air intake angle is 2.5° , the air outlet angle is 2.5° , the battery intervals adopt an equally spaced flow channel layout, and the maximum temperature and temperature difference of the system reach the minimum values, indicating that the heat dissipation effect of the air-cooling system is better at this time. Yu et al. [89] developed a three-dimensional numerical model based on the Bernard model, integrating the measured data of the thermal physical properties of materials, the internal resistance of the battery, and the volt-temperature coefficient to characterize the battery's discharge heat behavior. Moreover, they designed a bidirectional airflow thermal management system. Figure 9a,b is a schematic diagram of the system structure. This system integrates structures such as the main air duct, vertical turning air duct, and jet holes. The cooling airflow of each air duct can be independently configured and supplied by a single or multiple fans. According to the results shown in Figure 9c,d, the maximum temperature of the battery pack with the bidirectional airflow design is reduced by at least $9\text{ }^\circ\text{C}$ compared with the initial battery pack temperature, and the heat accumulation of the intermediate unit is greatly improved. The maximum temperature difference within each unit does not exceed $5\text{ }^\circ\text{C}$. It can be seen from this that the bidirectional airflow design greatly improves the cooling efficiency of the intermediate battery. The bottom channel can significantly reduce the battery temperature, and the two independent air duct designs avoid mutual interference between fans. This thermal management system design is conducive to improving the overall air-cooling efficiency, extending the battery life, and meeting the high reliability requirements of the system.

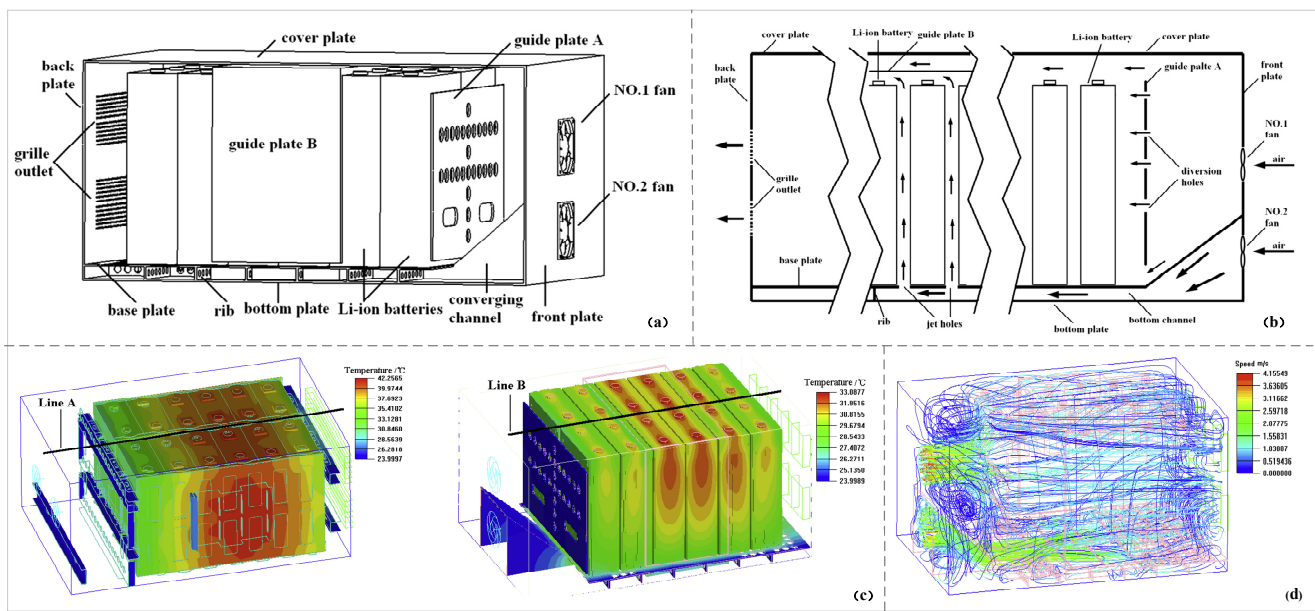


Figure 9. (a) Three-dimensional diagram of the two-directional air flow cooling pack; (b) side view of the two-directional air flow cooling pack; (c) comparison of temperature contour lines at the end of 1C rate discharge between the original group and the two-directional air flow cooling pack; (d) streamline in the two-directional air flow cooling pack (Adapted with permission from Ref. [89]).

4.2. Liquid Cooling Technology

Liquid cooling technology is a technology that connects energy storage equipment with a liquid cooling system, uses high thermal conductivity liquid such as water and ethanol as a heat transfer medium, and takes away heat through indirect contact between the diversion groove on the liquid cooling plate and the battery core so as to cool the battery. Compared with the air-cooling system, the liquid cooling system has a more compact structure, a small footprint, good heat dissipation, and high safety. However, the liquid cooling system also has the problems of complex installation, high cost, and high energy consumption [90]. According to the contact mode of the coolant and the energy storage equipment, the liquid cooling technology is divided into two categories: direct liquid cooling and indirect liquid cooling. Direct liquid cooling refers to the direct immersion of hot electronic components in insulating and chemically inert coolant, and the heat generated is taken away through the continuous circulation of coolant. This method has high refrigeration efficiency, but it has high requirements on the sealing and insulation of electronic components. The representative technology is immersion liquid cooling technology. In indirect liquid cooling, the heating element does not directly come into contact with the cooling medium but dissipates heat through the contact of the cold plate with liquid, or the heat is transferred to the cold plate by the heat conduction component, and the heat is taken away by the liquid circulation inside the cold plate. Indirect liquid cooling technology is relatively mature, and the cost of transformation is low, but the heat dissipation efficiency is slightly lower than that of direct liquid cooling. The representative technology is cold plate liquid cooling technology.

Zhang et al. [91] conducted numerical simulation and comparative analysis on the thermal performance of straight-through channel cold plates and inclined channel cold plates under different coolants, channel numbers, and mass flow conditions and conducted experimental research on inclined channel cold plates based on a simplified streamlined structure. The specific structure is shown in Figure 10a. In the experiment, water, mineral oil, and a water–ethanol mixture were selected as cooling media to compare the heat transfer performance of the two types of cold plates under different coolant conditions. As shown

in Figure 10c, despite the different types of coolants used, the heat transfer coefficient of the straight-through channel cold plate changes slightly, while the heat transfer coefficient of the inclined channel cold plate is significantly improved, indicating that the structure has better heat transfer capacity under the action of various coolants.

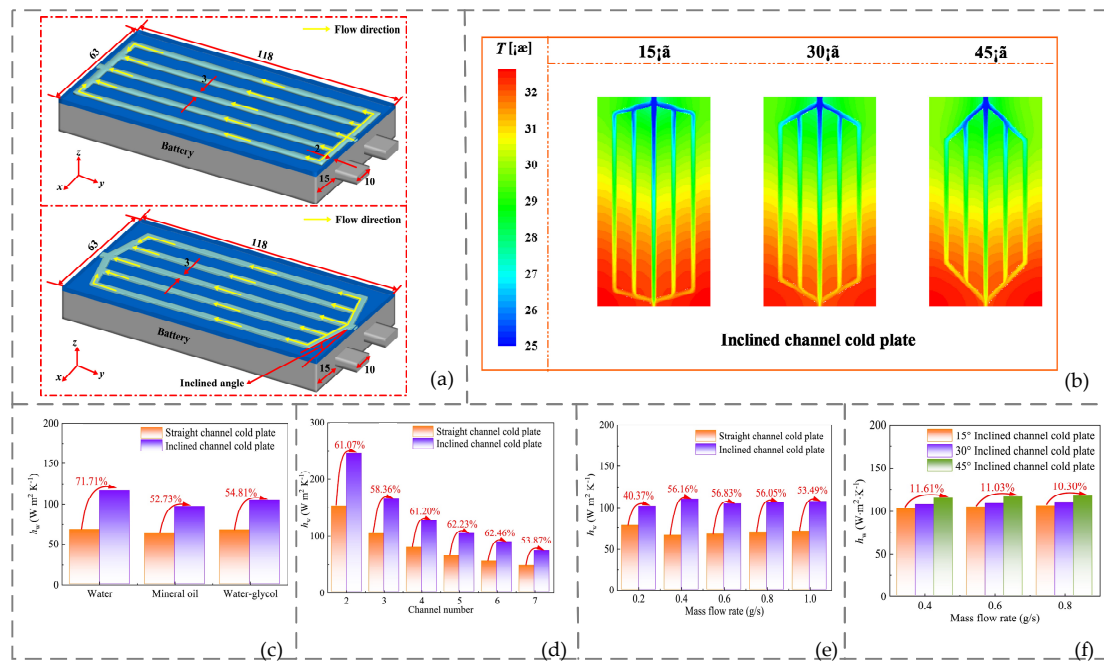


Figure 10. (a) Schematic diagram of a prismatic battery with cold plate. (b) Effects of inclined angle on the temperature distribution of the inclined channel cold plate. (c) The influence of coolant on the heat transfer coefficient. (d) The influence of the channel number on the heat transfer coefficient. (e) The influence of mass flow rate on the heat transfer coefficient. (f) The influence of inclined angle on the heat transfer coefficient (Adapted with permission from Ref. [91]).

In addition, Figure 10d shows the effect of the number of channels on the thermal performance of the two cold plates. The study shows that with the increase in the number of channels, the heat transfer coefficients of the straight-through channel cold plate and the inclined channel cold plate both show a downward trend. However, under the condition of the same number of channels, the heat transfer coefficient of the inclined channel cold plate is always higher than that of the straight channel cold plate, and the improvement can exceed 53%, indicating that the inclined design has higher heat dissipation efficiency under multi-channel configuration.

Further, Figure 10e explores the effect of mass flow rate on the thermal performance of the cold plate. In a structure with five channels and an inclination angle of 15°, water was used as the cooling medium for testing. The results show that with an increase in the mass flow rate, the heat transfer coefficients of the two types of cold plates change, but the fluctuation is small, and when the flow rate exceeds 0.2 g/s, the advantage of the inclined channel cold plate in heat transfer enhancement tends to be stable.

Finally, as shown in Figure 10f, the change in the inclination angle also has a significant effect on the performance of the inclined channel cold plate. Under the same mass flow rate, an increase in the inclination angle will increase the heat transfer coefficient of the cold plate, indicating that a larger inclination angle helps enhance heat transfer under low-flow conditions. However, as shown in Figure 10b, a too-large inclination angle may lead to uneven cooling at the corners of the cold plate, thus affecting the temperature consistency and thermal management effect in practical applications. Therefore, the heat transfer

efficiency and the balance of temperature distribution must be considered comprehensively during design.

Furthermore, Yao et al. [92] proposed an optimization design method for power conversion system (PCS) liquid cooling heat sinks based on the multi-objective gray wolf optimization algorithm for an environment with low air density, low pressure, and weak convection in high-altitude areas. The heat sink flow channels adopt a snake-shaped design, and the best heat dissipation performance is achieved by continuously optimizing relevant data, such as the width and height of the flow channels. It is concluded through simulation and experiments that this design method can greatly improve the heat dissipation performance of the radiator.

Zeng et al. [93] conducted research on immersion cooling technology, reviewed the significant advantages of immersion cooling technology over traditional thermal management technology in terms of temperature control performance and energy efficiency, and summarized five commonly used dielectric fluids, namely electronic fluorinated fluids, hydrocarbons, esters, silicone oils, and water-based fluids, from the perspectives of thermal conductivity, safety, and economy. The system compared the advantages and disadvantages of different fluids, and the comparison of each index is shown in Figure 11.

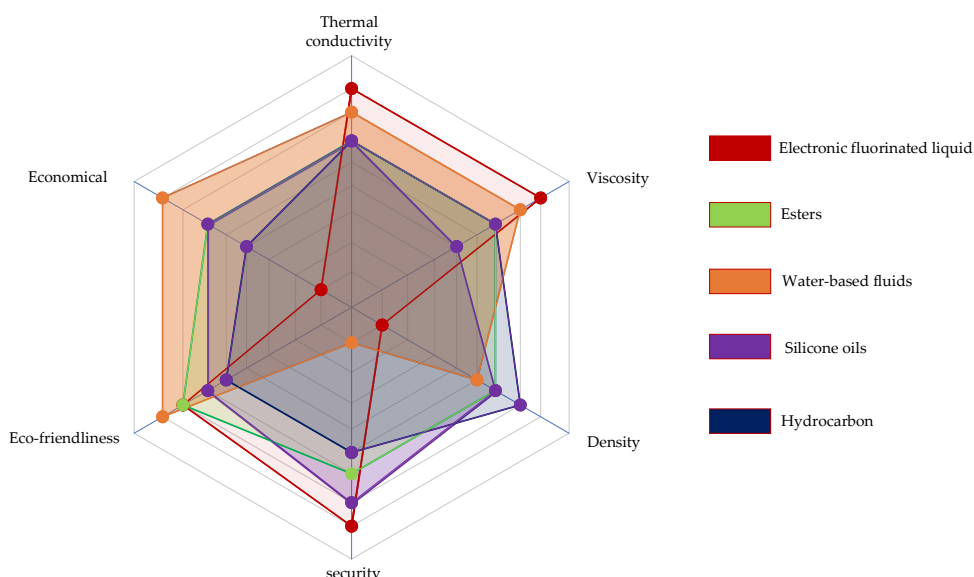


Figure 11. Comparison of dielectric fluid specifications (Adapted with permission from Ref. [93]).

4.3. Phase-Change Cooling Technology

Phase-change cooling technology is a cooling method that utilizes the phase change of phase-change materials to absorb heat. The phase-change materials themselves do not have the ability to dissipate heat, and the absorbed heat needs to be discharged through liquid cooling systems, air cooling systems, etc. Otherwise, the phase-change materials cannot continuously absorb heat. The specific principle is shown in Figure 12. Phase-change cooling is a passive thermal management strategy, which has the advantages of simple structure, lightweight design, high performance, and no need for additional auxiliary equipment [94].

Yuan et al. [95] developed a cascade energy storage phase-change cooling system based on the vapor compression refrigeration cycle in response to the special requirements of the cooling system for high-power electronic equipment operating intermittently. The system consists of two independent cycles. The first-stage cooling system drives the working medium cycle through a mechanical pump to transfer heat from the electronic equipment to the energy storage device. The secondary cooling system utilizes the traditional vapor

compression refrigeration cycle to store cold in the energy storage device. By comparing the physical properties of different working fluids, it is found that NH_3 has a high latent heat and a small gas–liquid density ratio, which is conducive to reducing the mass flow rate and pressure fluctuations in the system cycle. Therefore, NH_3 was selected as the working fluid for the primary cycle. Through experimental verification, key parameters, such as the cooling capacity, pressure variation, and temperature distribution of the test system, under different heat loads were tested. It was confirmed that the designed energy storage phase-change cooling system meets the cooling requirements of short-term high-power electronic equipment, can effectively control temperature fluctuations, reduce the area of the cooler and the volume of the system, and achieve the development goals of energy conservation and miniaturization.

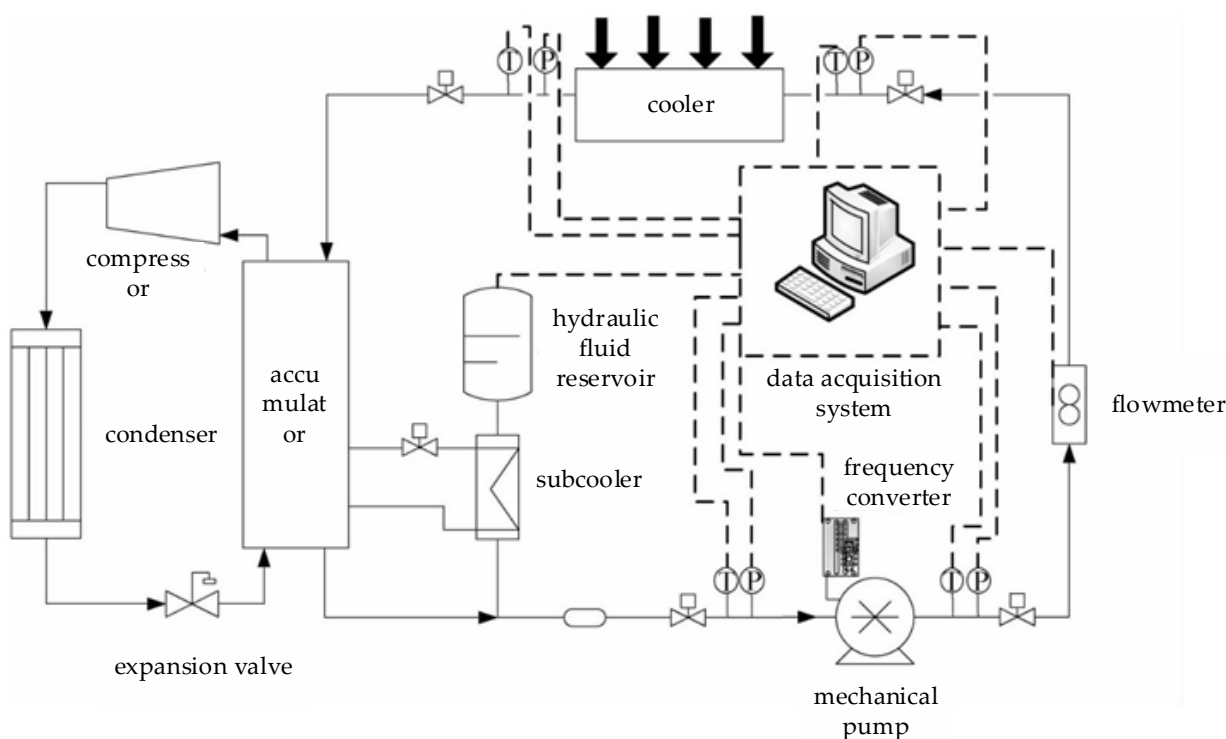


Figure 12. Principle of phase-change cooling system (Adapted with permission from Ref. [95]).

Andrew et al. [96] designed a passive thermal management system using phase-change material (PCM). PCM absorbs and stores heat during the phase transition process, which can minimize the temperature change of the battery pack. Through experimental measurement of the heat generation rate of lithium-ion batteries under different power discharges, it was found that the heat generation rate increased with the increase in discharge power. Moreover, the experimental results show that the use of phase-change material/expanded graphite (PCM/EG) composite materials can significantly improve the thermal conductivity. Finally, through experiments and simulations, it is found that increasing the volume of the battery pack and the usage of PCM can significantly improve the performance of the thermal management system.

Li et al. [97] conducted a study on aluminum foamer–polyethylene glycol phase-change energy storage materials. By the vacuum impregnation method, polyethylene glycol (PEG)-based phase-change energy storage materials were prepared with aluminum foam as the encapsulation carrier. After the Comsol simulation, the performance was consistent with that during the experiment, proving that the thermal conductivity of the composite phase-change material was superior to that of PEG. It can rapidly absorb the uneven high temperature on the battery surface, thereby extending the battery's service life.

Zheng et al. [98] studied the significant role of hydrated salt phase-change materials in the thermal management of lithium-ion batteries. They prepared a phase-change material composed of eutectic hydrated salts made up of sodium acetate trihydrate, glycine, disodium hydrogen phosphate dodecahydrate, and expanded graphite. The research found that when the addition amount of expanded graphite was 10%, the phase-change temperature of the material was 45.31 °C. The enthalpy of phase change is 196.17 J/g, and the thermal conductivity is 1.60 W/(m·K), which has a good anti-leakage ability. Under an environment of 25 °C, when using this phase-change material for cooling, when the discharge rate is 2C, the maximum temperature difference of a single cell is only 0.21 °C, the maximum temperature of the battery pack is controlled within 55 °C, and the maximum temperature difference between battery packs is 2.41 °C, which is reduced by 89.55%, 22.24%, and 77.46%, respectively, compared with air cooling. This indicates that the hydrated salt phase-change material can effectively improve the temperature uniformity of the battery pack during high-rate discharge, keeping it within an appropriate temperature range.

Based on comprehensive data analysis, the characteristics of different battery thermal management technologies are shown in the following Table 5. Judging from their advantages, disadvantages, and application scopes, liquid cooling technology has a wide range of adaptability and is more mature. It is currently a commonly adopted thermal management technology in energy storage power stations.

Table 5. Characteristics of different battery thermal management solutions [99–103].

Item	Air Cooling	Liquid Cooling	Phase-Change Cooling	Typical Quantitative Metrics
Heat dissipation efficiency	mid	high	high	Air: 30–100 W; Liquid: 200–500 W; Phase Change: >500 W
Heat removal rate	mid	pronounced	pronounced	Air: ~0.5–2 W/cm ² ; Liquid: ~5–10 W/cm ² ; Phase: ~10–15 W/cm ²
Temperature drop	mid	pronounced	high	Air: $\Delta T \approx 8\text{--}12^\circ\text{C}$; Liquid: $\Delta T \approx 3\text{--}5^\circ\text{C}$; Phase: $\Delta T \approx 4\text{--}6^\circ\text{C}$
Temperature difference	pronounced	cataphyll	cataphyll	
Complexity	mid	pronounced	mid	
Cost	longevity	mid	longevity	
Technology maturity	maturity	maturity	becoming mature	
Lifetime	cataphyll	pronounced	pronounced	
Commercial application	commercially available	commercially available	not yet	

5. Fire Extinguishing Technology for Energy Storage Power Stations

Battery thermal runaway often leads to the occurrence of fires. When a fire breaks out, how to eliminate it is currently a hot topic of research among experts and scholars. Among them, the research on fire extinguishing agents and fire extinguishing strategies is a key area of concern. This chapter mainly reviews the suppression effect of typical fire extinguishing agents on fires in lithium battery energy storage power stations and introduces the current popular fire extinguishing strategies and research progress.

5.1. Types of Fire Extinguishing Agents

5.1.1. Water-Based Fire Extinguishing Agent

The water-based fire extinguishing agents commonly used for fire suppression in energy storage power stations mainly include fine water mist, fine water mist containing additives, and hydrogel. The fire extinguishing mechanism of pure water fine water mist is shown in Figure 13. Its main limitations lie in the fire extinguishing effect and

application scope. To enhance the fire extinguishing efficiency of fine water mist, many experts and scholars have developed fine water mist containing additives. The main function of additives is to change the properties of water. Physical additives can increase the vaporization heat absorption and wetting capacity of water. Water can absorb more heat released by the flame of the thermal runaway battery through its own vaporization reaction, thereby reducing the temperature of the thermal runaway battery and the adjacent battery pack. Chemical additives react to release inert gases, which can undergo decomposition reactions at certain temperatures to release nitrogen-containing compounds. A sudden increase in the content of inert gases can reduce the volume fraction of oxygen in the reaction zone, isolating combustibles from oxygen and achieving the effect of suffocation and fire extinguishing.

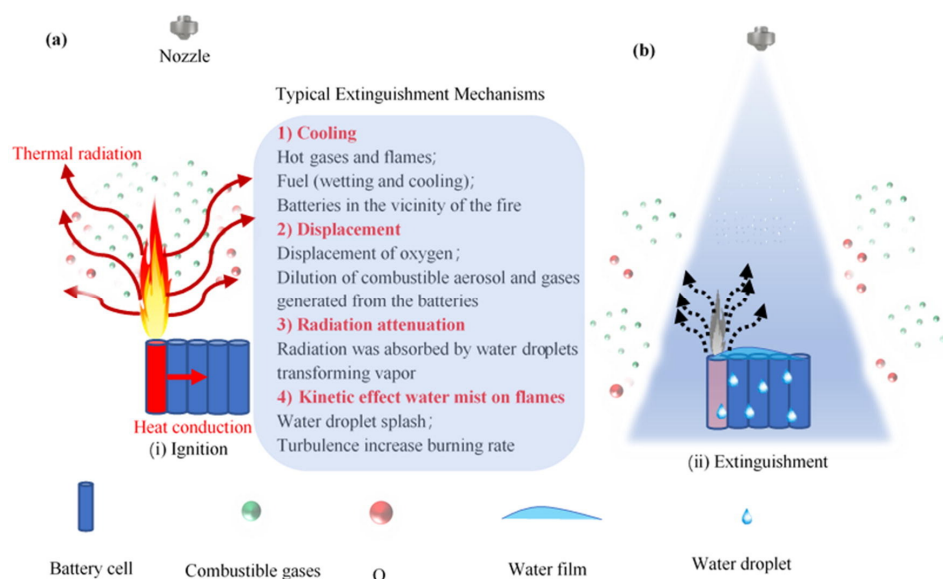


Figure 13. Extinguishing mechanisms of water mist (WM) on LIB fires. (a) Typical ignition and propagation of LIBs and (b) extinguishment of LIB fire under water mist conditions (Reprinted with permission from Ref. [104]).

Liu et al. [105] compared the key performance of water-formed foam fire extinguishing agents and water-based fire extinguishing agents in extinguishing liquid fires through experiments. Water-formed foam fire extinguishing agents were superior to water-based fire extinguishing agents in key performance indicators such as surface tension, interfacial tension, foaming multiple, and 25% liquid separation time. In the fire extinguishing performance test, water-formed foam fire extinguishing agents demonstrated shorter fire extinguishing times and longer reignition times. They could quickly extinguish the flames and form a dense foam layer on the fuel surface, effectively preventing reignition. In contrast, most water-based fire extinguishing agents failed to completely extinguish the fire within the specified time, leaving residual flames and having poor anti-reignition performance.

Ji et al. [106] conducted a numerical simulation of the effect of water spray on suppressing fires in lithium-ion batteries. The research finds that water spray achieves fire extinguishing through multiple mechanisms, such as surface cooling, oxygen isolation, heat radiation blocking, and wetting of the burning material. Through the analysis of the simulation results, the following conclusions are drawn: The fire-extinguishing effect of water spray is influenced by multiple factors. The greater the spray flow rate and the lower the initial velocity, the better the fire extinguishing effect. Moreover, increasing the nozzle height, optimizing the installation angle, and increasing the number of nozzles can also significantly enhance the fire extinguishing efficiency. In addition, early spray initiation and

extended spray duration help to better control the fire, lower the maximum temperature of the battery pack, and thereby effectively curb the spread of the fire.

Zhang et al. [107] studied the delaying effect of fine water mist containing nonionic surfactants on the thermal runaway of lithium batteries. By adding three nonionic surfactants, FS 3100, Tween 80, and APG 0810, to the fine water mist, they compared and analyzed the effects of different additives on the suppression of thermal runaway of lithium batteries by fine water mist. The article compared the cooling effects of the three. APG 0810 performed best in improving the cooling effect of fine water mist, shortening the cooling time to 223 s, followed by Tween 80, and FS 3100 had the worst effect. Additionally, Tween 80 was found to be the most effective additive, reducing the maximum thermal runaway temperature to 539.9 °C and decreasing the average heating rate. Subsequently, through the analysis of the cooling mechanism, it was found that APG 0810 enhanced the wettability and evaporation heat absorption capacity of the battery by reducing the surface tension and contact angle of the fine water mist, while Tween 80 effectively inhibited the thermal runaway and temperature rise of the battery by improving the foaming capacity and generating unstable foam, and the foam rupture carried away the heat. Finally, the article compared the influence of additives on the foam performance. The study found that Tween 80 had the highest foaming ability, but the foam stability was low, and it was prone to rupture, which was conducive to heat dissipation. The foam produced by APG 0810 has good stability, but it has a high liquid content, which is not conducive to heat dissipation. To further reduce the environmental load of chemical additives and improve the sustainability of fire extinguishing agents, recent studies have begun to focus on bio-derived polymer flame retardant systems. Kumar et al. [108] systematically evaluated the flame-retardant efficiency of bioactive natural polysaccharides and their secondary metabolites in textiles. It was found that these compounds could significantly inhibit the heat release rate in the range of 300–400 °C by catalyzing the synergistic mechanism of char formation and free radical capture, and their decomposition products were non-toxic and biodegradable. This result provides a new idea for the development of green water mist additives for lithium battery energy storage cabins: the combination of polysaccharide derivatives with existing non-ionic surfactants is expected to maintain efficient cooling while taking into account eco-friendliness and material compatibility. The long-term stability in high humidity and high salt fog environments and the interaction with battery materials need to be studied in the future.

5.1.2. Gas Fire Extinguishing Agent

In energy storage power stations, commonly used gaseous fire extinguishing agents include perfluorohexanone, heptafluoropropane, and carbon dioxide. Among them, heptafluoropropane is an excellent substitute for halogenated hydrocarbon fire extinguishing agents, with good environmental adaptability, low toxicity, short residual time, and excellent electrical insulation properties. Its fire extinguishing mechanism combines physical inhibition and chemical inhibition: the physical effect mainly depends on the cooling effect, and its decomposition process can absorb a certain amount of heat; in terms of chemical mechanism, the fluorine-containing free radicals produced by its decomposition can effectively capture free radicals, such as H·, ·O, and ·CH₃, thereby interrupting the combustion chain reaction [109].

Perfluorohexanone is a new type of clean gas fire extinguishing agent commercialized by 3M (The global headquarters of Minnesota Mining and Manufacturing Company is located in Saint Paul, MN, USA; It is a world-renowned diversified technology innovation enterprise) in 2001, which has both high efficiency and environmentally friendly characteristics. The substance has a large latent heat of evaporation and absorbs heat through

phase change to quickly reduce the flame temperature and achieve fire extinguishing. The chemical inhibition principle is mainly that the ·CF₃ and ·CF₂ free radicals produced by its pyrolysis can react with the H· and ·OH free radicals in the flame to generate more stable HF and CF₂O, thereby effectively blocking the combustion reaction chain [102]. Due to the advantages of being non-conductive, non-corrosive, and residue-free, these gaseous fire extinguishing agents are widely used in precision equipment and electrical fires.

Yu et al. [110] conducted a full flooding fire extinguishing experiment of heptafluoropropane on lithium iron phosphate cells and battery modules. By arranging thermocouples and gas analyzers in a specific experimental space, the fire extinguishing performance of the single cells and modules was tested. The experimental results show that at a concentration of 10% by volume, heptafluoropropane can quickly extinguish open flames, and no reignition occurs within a 20 min immersion period, but its inhibitory effect on battery thermal runaway still has certain limitations. This study shows that HFC-227ea has the initial ability to suppress lithium-ion battery fires and suggests that the fire can be further prevented from spreading by enhancing the isolation design between battery modules.

Xie et al. [111] constructed a lithium battery combustion and fire extinguishing test platform, used electric heating to induce thermal runaway of lithium-ion single cells, and systematically studied the fire extinguishing and cooling performance of perfluorohexanone. They measured the fire extinguishing time, maximum temperature, mass loss, and fire extinguishing efficiency under different experimental conditions. The results showed that under standard configuration, perfluorohexanone could quickly extinguish the flame, but when the concentration of the extinguishing agent was reduced, the battery might reignite within 60 s after the flame was extinguished.

Wang et al. [112] evaluated the fire extinguishing effect of heptafluoropropane on lithium titanate batteries (LTO). The experiment used electric heating to induce thermal runaway of LTO cylindrical batteries with a capacity of 50 Ah and 2.3 V. The fire extinguishing performance was analyzed by recording parameters such as temperature change, fire ignition time, fire extinguishing agent release time, extinguishing time, and mass loss. The results show that HFC-227ea can effectively extinguish single or small-scale battery module fires, but due to the violent reaction inside the battery, there is still a risk of reignition. Therefore, it is recommended to apply the fire extinguishing agent as early as possible and appropriately extend the spraying time to enhance the continuity of fire extinguishing. At the same time, the study pointed out that the effect of HFC-227ea concentration on the fire extinguishing efficiency of LTO batteries needs further in-depth discussion.

5.1.3. Solid Fire Extinguishing Agent

Solid fire extinguishing agents are mainly dry powders, which can be classified into ABC powder, BC powder, and D powder according to their components. They feature high fire extinguishing efficiency, convenient storage, low cost, and a wide application range [8].

Meng et al. [24] explored the fire extinguishing efficiency of dry powder fire extinguishing agents for lithium iron phosphate batteries under different SoCs by constructing an experimental platform. Experiments have found that dry powder fire extinguishing agents can put out fires under appropriate conditions, but they cannot prevent the exothermic reactions inside the battery. Therefore, the cooling effect on the parts of the battery that have not come into contact with the fire extinguishing agent is limited. Moreover, the fire extinguishing effect can be improved by shortening the spray distance and extending the spray time, while adjusting the spray angle has little impact on the fire extinguishing effect. Therefore, dry powder fire extinguishing agents should be used as early as possible. The required dry powder mass should be determined based on the operating conditions and capacity of the battery module.

5.1.4. Comparison of Typical Fire Extinguishing Agents

Some scholars have compared different types of fire extinguishing agents, hoping to select those with good fire extinguishing effects and economic rationality for fire suppression in energy storage power stations. Zhang et al. [23] studied the cooling effects of different fire extinguishing agents on lithium iron phosphate energy storage batteries after thermal runaway. Through experiments, they compared four fire extinguishing agents: nitrogen, heptafluoropropane, perfluoropropane, and fine water mist. The test results showed that fine water mist had the best cooling effect, and the cooling effects were in the order of fine water mist > perfluoropropane > heptafluoropropane > nitrogen. The cooling effect of nitrogen is comparable to that of the blank control group, with almost no cooling effect. Moreover, after the fire extinguishing agent is completely discharged at one time, the cooling effect can only last for about 20 min. If further cooling is desired, the fire extinguishing agent needs to be turned on multiple times.

Through the research and investigation of various literature, the characteristics of the water-based fire extinguishing agents, gas fire extinguishing agents, and solid fire extinguishing agents are compared as shown in the following Figure 14 and Table 6. Based on comprehensive data analysis, the existing fire extinguishing agents can quickly put out the open flames of batteries, but they have little effect in suppressing reignition. In experiments and actual engineering, it was found that the effect of the same fire extinguishing agent varies greatly at different thermal runaway chain reaction nodes, and the effect of different fire extinguishing agents also varies greatly at the same fire time node. At present, the problem of flame reignition is rather difficult to solve completely. When the battery catches fire, it is hard to extinguish the flame using water mist, which cannot effectively suppress the thermal runaway spread of the battery module. Therefore, the development of multiple fire extinguishing agent combination methods and efficient fire extinguishing methods is becoming the main research direction in the field of fire extinguishing for energy storage power stations.

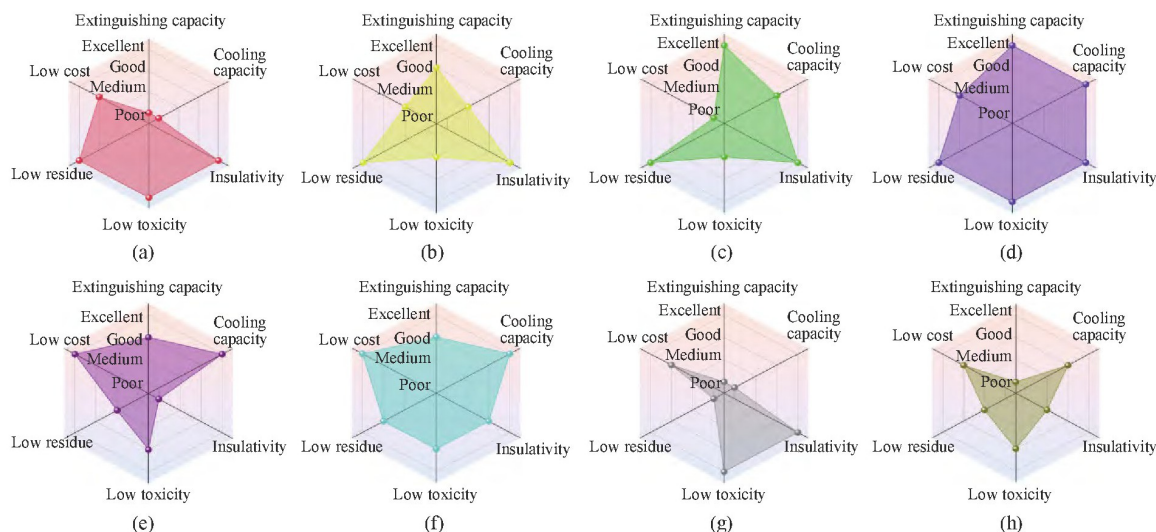


Figure 14. Radar map for performance evaluation of eight typical fire extinguishing agents: (a) CO₂; (b) HFC-227ea; (c) C₆F₁₂O; (d) liquid nitrogen; (e) water spray; (f) water mist; (g) foam; (h) dry powder (Adapted with permission from Ref. [104]).

Table 6. Comparison of main fire extinguishing agents [113,114].

Type of Fire Extinguishing Agent	Representative	Merit	Defect
Water-based fire extinguishing agent	water mist	Non-toxic, non-polluting, rapid fire extinguishing, high efficiency	Immersion into rechargeable batteries may cause thermal runaway.
	heptafluoropropane fire extinguishing agent	Less residue, low conductivity, and low toxicity.	In the early stage of fire extinguishing, a large amount of toxic gases such as hydrogen fluoride will be produced.
	perfluorohexanone extinguishing agent	It is harmless to equipment, clean, and environmentally friendly, and has a wide range of applications.	The manufacturing cost is high, and the preservation is difficult.
Gaseous fire extinguishing agent	CO ₂ fire extinguishing agent	Environmentally friendly, wide range of applications.	The fire cannot be extinguished. Even if the fire is extinguished, the battery will reignite and cannot be suppressed.
	dry chemical extinguishing agent	Quick, effective, and easy to operate	Does not have the cooling effect.
	aerosol fire extinguishing agents	Environmentally friendly, no pressure storage	Limited scope of application
Solid extinguishing agent			

5.2. Fire Extinguishing Strategies

5.2.1. Coordinated Fire Extinguishing with Multiple Fire Extinguishing Technologies

Given the varying physical and chemical properties of different fire suppression agents, relying on a single agent is often insufficient to fully extinguish lithium-ion battery fires. In practical applications, a hybrid approach that combines the strengths of multiple agents proves more effective. A representative strategy combining agents with strong cooling capabilities is illustrated in Figure 15a.

Zhang et al. [115] investigated the synergistic fire suppression effects of several gaseous agents—namely C₆F₁₂O (Novec 1230), CO₂, and HFC-227ea—when used in conjunction with water mist to suppress fires involving a 243 Ah lithium iron phosphate (LFP) battery. Key evaluation parameters included extinguishing time, peak temperature, battery mass loss, and heat release rate. The study comprehensively assessed the fire suppression performance, cooling capacity, and economic feasibility of different combinations. Results demonstrated that combining gaseous extinguishing agents with water mist significantly outperformed the use of single agents. In particular, the pairing of C₆F₁₂O with water mist achieved the most favorable fire suppression and cooling results. The CO₂–water mist combination also yielded strong performance in terms of both thermal control and cost-effectiveness. However, HFC-227ea alone failed to extinguish the flames effectively. These findings underscore that integrated fire suppression strategies can more effectively mitigate battery fires, limit thermal propagation, reduce mass loss, and delay the onset of thermal runaway.

In a separate study, Lu et al. [116] proposed a fluorine-based rapid suppression and passivation cooling technique aimed at preventing reignition in lithium battery energy storage systems. Their approach was validated through fire suppression experiments on large-scale battery modules. The proposed method successfully extinguished initial flames within seconds and prevented subsequent reignition. The study critically evaluated the pros and cons of conventional water- and gas-based fire suppression systems, highlighting that while fluorinated agents such as perfluorohexanone possess excellent flame-suppressing properties, their cooling effects remain suboptimal. To address this, a dual-agent strategy combining perfluorohexanone and low-pressure CO₂ was examined. Experimental results showed that flames could be extinguished within 5 s, and the continued intermittent release

of CO₂ significantly lowered the surrounding temperature, with minimum temperatures reaching -60°C . Notably, the low-pressure CO₂ penetrated the battery enclosure, where it reacted with lithium to form stable lithium carbonate compounds. This not only suppressed internal chemical reactions but also helped establish a passivation layer, effectively reducing the risk of reignition.

5.2.2. Intermittent and Multiple Fire Extinguishing Operations

To enhance the fire suppression and cooling performance of a single fire extinguishing agent, modifying the spray pattern is an effective approach to improve agent utilization efficiency. One such approach is the intermittent spray strategy, which controls the spray cycle and duty cycle to optimize the heat exchange and the cooling performance, as illustrated in Figure 15b.

Zhang et al. [117] conducted experiments to evaluate the impact of intermittent water spray cooling on thermal runaway in lithium-ion batteries. The study revealed that frequent short-cycle spraying can substantially lower the surface temperature of the battery and reduce post-extinguishment temperature rebound. Moreover, the results identified an optimal duty cycle that enhances cooling efficiency. The study also highlighted that the internal temperature of a battery undergoing thermal runaway, especially at 100% SOC, could exceed 1000°C , significantly higher than its surface temperature. Furthermore, the primary hazardous gases released during thermal runaway—CO and hydrogen fluoride (HF)—were found to increase in concentration with higher SOC levels. Notably, the use of water spray can exacerbate the toxicity of these gases, underscoring the necessity for stringent safety precautions when employing water-based suppression methods for lithium-ion battery fires.

Building on this, Meng et al. [118] proposed a novel fire suppression technique that integrates perfluorohexanone-based extinguishing agents with intermittent spray cooling (ISC) to address fires in lithium iron phosphate (LFP) batteries. Their experimental analysis investigated the effects of spray frequency and duty cycle on the cooling effectiveness. The results demonstrated that perfluorohexanone not only effectively suppressed LFP battery combustion but also significantly reduced toxic gas emissions and overall heat release. Compared to continuous spray methods, ISC was shown to prolong low-temperature conditions and slow the post-extinguishment temperature rise once the extinguishing agent had dissipated. Specifically, for 14 Ah LFP cells, the optimal duty cycle was determined to be 55.4%. The authors further noted that batteries with larger capacity or higher reactivity may require a higher optimal duty cycle to achieve superior fire suppression and thermal control.

5.2.3. Fire-Extinguishing Microcapsule Technology

Microcapsules are core-shell structures with polymers as the shell material and liquids or solids as the core material. The fire-extinguishing microcapsule technology provides a brand-new direction for the fire-extinguishing strategy of lithium batteries. The specific strategy is shown in Figure 15c.

Lou et al. [119] developed a new type of fire-responsive separator. By loading microcapsule fire extinguishing agents on the surface of the separator, when the battery experiences thermal runaway, the microcapsule shell automatically breaks to release the fire extinguishing agent, quickly absorbing heat and suppressing thermal runaway. Experiments show that batteries using this separator only produce smoke and no open flame during thermal runaway and can drop to room temperature within 20 s while maintaining good electrochemical performance.

Chinese patent CN109453491A [120] introduces the embedded new Halon alternative fire extinguishing agents, such as perfluorohexanone and heptafluoropropane, into urea-

formaldehyde or melamine resins. This invention features simplicity and low cost, and the fire extinguishing composition is highly reliable. After being made into the product, it does not require any power supply or dedicated smoke or temperature detectors. It does not require complex equipment or pipelines, integrating detection, control, start-up, and fire extinguishing units. It has good mechanical properties and anti-permeation performance. However, toxic formaldehyde gas is inevitably produced during the preparation process, which is harmful to human health.

At present, the research on the microencapsulation technology of liquid fire extinguishing agents at home and abroad is still in its infancy, and there are many problems. Better preparation processes need to be adopted to solve problems such as poor shell density, toxic gases in the process, and high production costs [121].

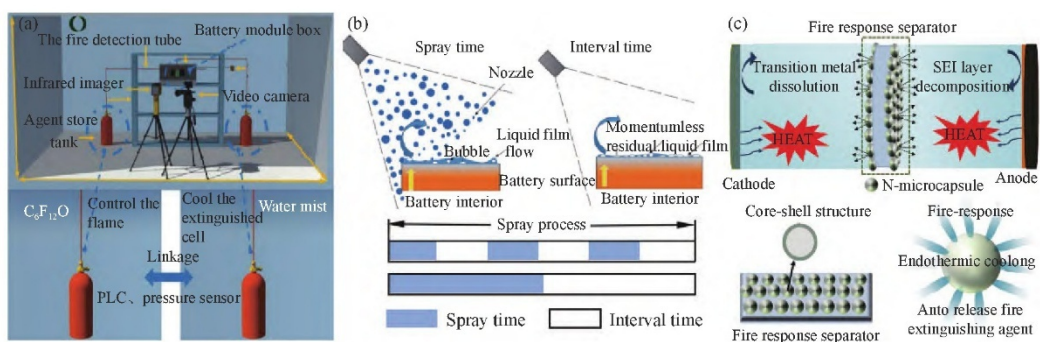


Figure 15. Schematic diagram of lithium battery fire extinguishing strategies (Adapted with permission from Ref. [8]): (a) collaborative fire extinguishing strategy (Adapted with permission from Ref. [122]); (b) intermittent spray strategy (Adapted with permission from Ref. [117]); (c) fire suppression microcapsule strategy (from Ref. [119] open access).

5.2.4. Thermal Safety Design of Material–Structure Integration

In addition to microcapsule fire extinguishing, another frontier path is to integrate the flame-retardant and heat-dissipation functions' 'original biochemistry' into the battery body. Wang et al. [123] uniformly embedded the expandable flame-retardant microspheres in the positive electrode and co-constructed them with a three-dimensional graphene thermal conductivity network to achieve a surface temperature rise of 0.2–3°C under full operating conditions. The fire was reduced by 42%, while maintaining an energy density of 93%; in the 200% SOC overcharge experiment, no fire or reignition was observed within 30 min. Although microcapsule fire extinguishing strategies (Section 5.2.3) and intermittent spray cooling (Section 5.2.2) demonstrate excellent fire extinguishing and temperature suppression performance at the laboratory scale, they are essentially "post-event" responses and cannot completely interrupt the thermal runaway chain reaction. This limitation stems from the fact that existing research separates material flame retardancy, structural heat dissipation, and thermal management strategies, resulting in a lack of synergistic effects between "material-level suppression" and "structural-level guidance." Therefore, this paper proposes to move thermal safety functions forward to the battery body design stage, constructing an integrated "material–structure–thermal safety" design paradigm to achieve source suppression and path blocking of thermal runaway.

Specifically, this paradigm leverages the phase-change cooling technology described in Section 4.3 as a bridge to deeply couple intrinsic material safety with structural thermal design. Drawing on the idea of embedding expanded flame-retardant microspheres (EFRMs) and three-dimensional graphene thermal conductive networks (3D-GNs) in electrodes by Wang et al. [123], by regulating the expansion temperature threshold of EFRMs (matching the SEI film decomposition temperature of 69 °C described in Section 2.2), a

dense carbon layer is formed at the early stage of thermal runaway, blocking the contact between oxygen and the electrolyte. At the same time, the lateral thermal conductivity of 3D-GNs (500 W/(m·K)) can quickly equalize the heat of local hot spots, avoiding the temperature gradient required for the “chain thermal runaway” described in Section 2.1.1. This provides more sensitive parameters for early warning. The ‘one stone two birds’ strategy shows that the electrode–structure integrated design can significantly weaken the thermal runaway chain reaction without sacrificing the energy performance, which provides a new material-level solution for the intrinsic safety upgrade of energy storage batteries.

6. Conclusions and Prospects

Electrochemical energy storage is an important part of future energy reforms. As the largest proportion of installed capacity in electrochemical energy storage, lithium battery energy storage has a huge space for development. In view of the possible thermal runaway problem of lithium battery energy storage power stations, this paper comprehensively reviews the characteristics and occurrence mechanism of lithium battery fires and summarizes the existing monitoring and early warning technologies, thermal management technologies, and fire extinguishing technologies of energy storage power stations. However, although these conclusions have become a consensus in the literature, they have not prevented a number of fires >100 MWh in recent years. The fundamental reason lies in the limitations of the experimental scale and operating conditions. The mainstream identification methods are mostly based on ≤10 Ah cells, and the module capacity involved in the literature [49,70] does not exceed 243 Ah, resulting in blind spots in the extrapolation of large-capacity system behavior. The main conclusions are as follows:

1. The monitoring and early warning technologies for lithium battery energy storage power stations can be classified into BMS monitoring and early warning and those based on internal temperature, characteristic gases, sound signals, expansion forces, and characteristic smoke images. Currently, the monitoring and early warning technologies for lithium battery energy storage power stations mainly include BMS monitoring and early warning, as well as those based on internal temperature, characteristic gases, sound signals, expansion forces, and characteristic smoke images. However, most of the existing early warning systems adopt single-parameter monitoring, resulting in unsatisfactory early warning effects. The existing system generally adopts the single-parameter criterion; the false alarm rate is high, and the early warning lag is obvious. As discussed in the review, Lyu et al. [37] coupled the acoustic MFCC characteristics with the hydrogen concentration information of Su et al. [67] and could issue an alarm 12 min before the occurrence of thermal runaway; they verified that the prototype had reached Technology Readiness Level (TRL) 7. Therefore, in the future, the multi-modal algorithm should be embedded into the edge AI chip along this path, and the extended interface should be reserved in the BMU-CAN bus of the 280 Ah standard module to realize the closed-loop of ‘detection-decision-action’ so as to compress the inherent 580 s lag of the single-parameter system to less than 60 s and complete the engineering leap from laboratory verification to the 1 MWh container.
2. After sorting out the current widely used thermal management technologies, it is found that they mainly cover three types of technologies: air-cooled, liquid-cooled, and phase-change cooling. Air-cooled technology dissipates heat with the help of air flow, which has the advantages of low cost and simple structure, but uneven heat dissipation can easily lead to temperature difference in the electric core, which damages the consistency and life of the battery; liquid-cooled technology dissipates heat with the circulation of coolant, which has a strong cooling capacity, but the system is complicated, heavy weight, difficult to maintain, and there are hidden

problems of liquid leakage; phase-change cooling technology absorbs heat with the help of phase-change materials, but the phase-change materials have poor thermal conductivity, which requires the addition of high-conductive materials, increasing costs. In the future, the development direction of thermal management technology should be intelligent, integrated, and efficient, and it is necessary to integrate different technologies and innovations to improve performance. Specifically, to bridge the gap between “laboratory verification and engineering scale”, the next stage should be to integrate the PCM/EG cold plate that Zheng et al. [96] have proven to reduce ΔT by 89% with the bidirectional air/liquid hybrid topology of Yu et al. [87] and build a “phase change-microchannel” integrated cold plate in the 280 Ah standard module, with a focus on completing aging verification with a leakage rate of <1% after 500 cycles; at the same time, the advantages of “liquid cooling 3–5 °C ΔT ” and “phase change 4–6 °C ΔT ” listed in Summary Table 5 should be coupled, and two-stage thermal control of first phase-change heat absorption and then liquid heat dissipation should be achieved in the same cold plate through a shared flow channel, thereby achieving a leap from single technology optimization to system-level reliability.

3. Commonly used extinguishing agents for lithium battery fires have been compared in the preceding sections with respect to the mechanism and effectiveness. Water-based systems exploit evaporative cooling and oxygen dilution, achieving rapid temperature reduction but showing a 40% short-circuit probability and a >60% reignition rate under the 243 Ah module tests reported by Zhang et al. [114]. Gaseous agents such as C₆F₁₂O and HFC-227ea extinguish open flames within 5 s via radical quenching, yet their limited cooling capacity leaves internal short circuits active, leading to flame reappearance within 60 s once concentration decays [108]. Solid (dry chemical) agents disrupt the combustion chain but exhibit uneven distribution and negligible heat extraction, as confirmed in Meng et al.’s LFP experiments [110]. Collectively, these shortcomings—insufficient cooling, high reignition probability, and toxic by-product formation—highlight the need for a paradigm shift from single-agent suppression to integrated strategies. The next step is to solidify the verified C₆F₁₂O–water mist synergistic strategy [114] into an engineering standard: prefabricate a dual-medium pipeline network in a 100 MWh container, extinguish the flame in the first round of 5% C₆F₁₂O in 5 s, and then intermittently cool with 0.3 MPa water mist for 15 min to suppress reignition, thus completing the leap from prototype verification to large-scale application.

Funding: This work is supported by the China Engineering and Technology Development Strategy Henan Research Institute Consulting Research Project (No. 2024HENZDB05), the Science and Technology Attack and Difficulties Program of Henan Province (No. 242102321108), and the Key Research and Development Special Project of Henan Province (No. 241111322400).

Data Availability Statement: This study’s original contributions are detailed in this article; any further inquiries can be addressed to the corresponding author.

Conflicts of Interest: The author declares no conflicts of interest.

References

1. China Energy Storage Alliance (CNESA). Energy Storage Industry White Paper 2025 (Summary Version). 2025. Available online: <https://static1.squarespace.com/static/55826ab6e4b0a6d2b0f53e3d/t/6822ec4402799548d7204853/1747119176770/Energy+Storage+Industry+White+Paper+Summary+2025+.pdf> (accessed on 3 August 2025).
2. Palizban, O.; Kauhaniemi, K. Energy Storage Systems in Modern Grids—Matrix of Technologies and Applications. *J. Energy Storage* **2016**, *6*, 248–259. [[CrossRef](#)]

3. Han, X.; Liu, Z. Research on Frequency Modulation Capacity Configuration and Control Strategy of Multiple Energy Storage Auxiliary Thermal Power Unit. *J. Energy Storage* **2023**, *73*, 109186. [[CrossRef](#)]
4. Guney, M.S.; Tepe, Y. Classification and Assessment of Energy Storage Systems. *Renew. Sustain. Energy Rev.* **2017**, *75*, 1187–1197. [[CrossRef](#)]
5. Wang, J.; Yu, Z.; Chu, X.; Wan, X.; Liu, Q. Research progress in safety characteristics of Li-ion batteries. *Battery Bimon.* **2003**, *33*, 388–391. [[CrossRef](#)]
6. Mahmood, N.; Tang, T.; Hou, Y. Nanostructured Anode Materials for Lithium Ion Batteries: Progress, Challenge and Perspective. *Adv. Energy Mater.* **2016**, *6*, 1600374. [[CrossRef](#)]
7. Ouyang, D.; Chen, M.; Huang, Q.; Weng, J.; Wang, Z.; Wang, J. A Review on the Thermal Hazards of the Lithium-Ion Battery and the Corresponding Countermeasures. *Appl. Sci.* **2019**, *9*, 2483. [[CrossRef](#)]
8. Huang, J.; Jin, J.; Zhao, L.; Liang, J.; Chen, Y. Review of fire extinguishing agents and fire suppression strategies for lithium-ion battery fire. *Chin. J. Eng.* **2024**, *46*, 2121–2132. [[CrossRef](#)]
9. Tao, Z.; Zhu, S.; Hou, S.; Li, K.; Wang, H. Comprehensive research on fire and safety protection technology for lithium battery energy storage power stations. *Energy Storage Sci. Technol.* **2024**, *13*, 536–545. [[CrossRef](#)]
10. Ghiji, M.; Novozhilov, V.; Moinuddin, K.; Joseph, P.; Burch, I.; Suendermann, B.; Gamble, G. A Review of Lithium-Ion Battery Fire Suppression. *Energies* **2020**, *13*, 5117. [[CrossRef](#)]
11. Qian, Y.; Zuo, F.; Ye, J.; Wang, H. Analysis of thermal runaway mechanism of lithium-ion battery and research on control method. *Chin. J. Power Sources* **2022**, *46*, 1227–1232. [[CrossRef](#)]
12. Shen, D.; Zhang, L. Thermal Runaway Mechanism and Existing Solutions for Lithium-Ion Batteries. *J. Adv. Phys. Chem.* **2024**, *13*, 607–615. [[CrossRef](#)]
13. Chen, S.; Bai, Y. Thermal Runway Mechanism and Research Progress on Thermal Management of Lithium-ion Power Batteries. *Bull. Natl. Nat. Sci. Found. China* **2023**, *37*, 187–198. [[CrossRef](#)]
14. Xu, H.; Zhang, X.; Xiang, G.; Li, H. Optimization of Liquid Cooling and Heat Dissipation System of Lithium-Ion Battery Packs of Automobile. *Case Stud. Therm. Eng.* **2021**, *26*, 101012. [[CrossRef](#)]
15. Aan, F.; Zhao, H.; Cheng, Z.; Yi-cheng, Q.J.; Zhou, W.; LI, P. Development status and research progress of power battery for pure electric vehicles. *Chin. J. Eng.* **2019**, *41*, 22–42. [[CrossRef](#)]
16. Geng, L.; Zhao, Y.; Gao, N.; Chen, Y. Review of Short-Circuit Formation Mechanisms and Diagnostic Methods in Lithium-Ion Batteries. *Chin. J. Automot. Eng.* **2023**, *13*, 481–495.
17. Wu, A.; Tabaddor, M.; Wang, C.; Jeevarajan, J. Simulation of internal short circuits in lithium ion cells. In Proceedings of the 2013 IEEE Transportation Electrification Conference and Expo (ITEC), Detroit, MI, USA, 16–19 June 2013; pp. 1–6. [[CrossRef](#)]
18. Jana, A.; Ely, D.R.; García, R.E. Dendrite-Separator Interactions in Lithium-Based Batteries. *J. Power Sources* **2015**, *275*, 912–921. [[CrossRef](#)]
19. Zhu, J.; Feng, J. In situ observation of lithium dendrite on the electrode in a lithium-ion battery. *Energy Storage Sci. Technol.* **2015**, *4*, 66–71. [[CrossRef](#)]
20. Gou, Q.; Xu, J.; Meng, N. Research Progress on Internal Short Circuit of Lithium-ion Battery. *Small Intern. Combust. Engine Motorcycle* **2022**, *51*, 89–92. [[CrossRef](#)]
21. Ren, D.; Feng, X.; Liu, L.; Hsu, H.; Lu, L.; Wang, L.; He, X.; Ouyang, M. Investigating the Relationship between Internal Short Circuit and Thermal Runaway of Lithium-Ion Batteries under Thermal Abuse Condition. *Energy Storage Mater.* **2021**, *34*, 563–573. [[CrossRef](#)]
22. Wang, G.; Ping, P.; Kong, D.; Peng, R.; He, X.; Zhang, Y.; Dai, X.; Wen, J. Advances and Challenges in Thermal Runaway Modeling of Lithium-Ion Batteries. *Innovation* **2024**, *5*, 100624. [[CrossRef](#)]
23. Zhang, H. Study of thermal runaway cooling of lithium iron phosphate energy storage battery under the action of liquid and gas extinguishing agents. *Chin. J. Power Sources* **2023**, *47*, 1046–1049. [[CrossRef](#)]
24. Meng, X.; Yang, K.; Zhang, M.; Gao, F.; Liu, Y.; Duan, Q.; Wang, Q. Experimental Study on Combustion Behavior and Fire Extinguishing of Lithium Iron Phosphate Battery. *J. Energy Storage* **2020**, *30*, 101532. [[CrossRef](#)]
25. Wang, C.; Gong, L.; Kang, P.; Tan, Y.; Li, M. Research on early warning system of lithium ion battery energy storage power station. *Energy Storage Sci. Technol.* **2018**, *7*, 1152. [[CrossRef](#)]
26. Chen, M.; Dongxu, O.; Cao, S.; Liu, J.; Wang, Z.; Wang, J. Effects of Heat Treatment and SOC on Fire Behaviors of Lithium-Ion Batteries Pack. *J. Therm. Anal. Calorim.* **2019**, *136*, 2429–2437. [[CrossRef](#)]
27. Yu, H.; Zhang, Y. Research progress of thermal runaway prevention and control technology for lithium battery energy storage systems. *Energy Storage Sci. Technol.* **2022**, *11*, 2653–2663. [[CrossRef](#)]
28. Lian, N.; Ji, W.; Chen, J. Research on the Safety Risk Analysis Framework and Control System for Multi-Type New Energy Storage Technologies. *Energies* **2025**, *18*, 798. [[CrossRef](#)]
29. McCoy, C.H. System and Methods for Detection of Internal Shorts in Batteries. Canadian Patent CA20142905013, 18 December 2014.

30. Jin, Y.; Xue, X.; Jiang, X.; Lv, N. Research Progress of Safety Protection of Lithium-ion Energy Storage Power Station. *J. Zhengzhou Univ. (Nat. Sci. Ed.)* **2023**, *55*, 1–13. [[CrossRef](#)]
31. Feng, X. Thermal Runaway Initiation and Propagation of Lithium-Ion Traction Battery for Electric Vehicle: Test, Modeling and Prevention. Ph.D. Thesis, Tsinghua University, Beijing, China, 2016.
32. Yang, Q.; Ma, H.; Duan, D.; Yan, J. Thermal runaway online warning method for lithium-ion battery based on gas characteristics. *High Volt. Eng.* **2022**, *48*, 1202–1211. [[CrossRef](#)]
33. Li, Z.; Li, X.; Wang, J.; Yang, L.; Zhang, Y.; Yan, T. Research Progress on Thermal Runaway Warning and Protection of Lithium-ion Battery in Energy Storage Power Station. *High Volt. Appar.* **2024**, *60*, 87–99. [[CrossRef](#)]
34. Su, T.; Lyu, N.; Zhao, Z.; Wang, H.; Jin, Y. Safety Warning of Lithium-Ion Battery Energy Storage Station via Venting Acoustic Signal Detection for Grid Application. *J. Energy Storage* **2021**, *38*, 102498. [[CrossRef](#)]
35. Raghavan, A.; Kiesel, P.; Sommer, L.W.; Schwartz, J.; Lochbaum, A.; Hegyi, A.; Schuh, A.; Arakaki, K.; Saha, B.; Ganguli, A.; et al. Embedded Fiber-Optic Sensing for Accurate Internal Monitoring of Cell State in Advanced Battery Management Systems Part 1: Cell Embedding Method and Performance. *J. Power Sources* **2017**, *341*, 466–473. [[CrossRef](#)]
36. Srinivasan, R.; Demirev, P.A.; Carkhuff, B.G. Rapid Monitoring of Impedance Phase Shifts in Lithium-Ion Batteries for Hazard Prevention. *J. Power Sources* **2018**, *405*, 30–36. [[CrossRef](#)]
37. Lyu, N.; Jin, Y.; Xiong, R.; Miao, S.; Gao, J. Real-Time Overcharge Warning and Early Thermal Runaway Prediction of Li-Ion Battery by Online Impedance Measurement. *IEEE Trans. Ind. Electron.* **2022**, *69*, 1929–1936. [[CrossRef](#)]
38. Rao, Z.; Lyu, P.; Li, M.; Liu, X.; Feng, X. A Thermal Perspective on Battery Safety. *Nat. Rev. Clean Technol.* **2025**, *1*, 511–524. [[CrossRef](#)]
39. Zhengzhou University. Early Safety Warning Method and Device for Lithium Batteries Based on Hydrogen Detection. Chinese Patent CN202010897596.5, 9 September 2022.
40. Lyu, N.; Jin, Y.; Miao, S.; Xiong, R.; Xu, H.; Gao, J.; Liu, H.; Li, Y.; Han, X. Fault Warning and Location in Battery Energy Storage Systems via Venting Acoustic Signal. *IEEE J. Emerg. Sel. Top. Power Electron.* **2023**, *11*, 100–108. [[CrossRef](#)]
41. Li, W.; Yang, F.; Wang, K.; Wu, X.; Ling, M.; Shen, X.; Yang, X.; Lin, Z.; Wu, K.; Liang, C. Clarifying the Effect of Pressure on Performance in Lithium-Ion Batteries. *J. Electrochem. Soc.* **2025**, *172*, 010512. [[CrossRef](#)]
42. Cummings, S.R.; Swartz, S.L.; Frank, N.B.; Dawson, W.J.; Hill, D.M.; Gully, B.H. Systems and Methods for Monitoring for a Gas Analyte. US Patent US15637381, 1 April 2018.
43. Wang, K.; Ouyang, D.; Qian, X.; Yuan, S.; Chang, C.; Zhang, J.; Liu, Y. Early Warning Method and Fire Extinguishing Technology of Lithium-Ion Battery Thermal Runaway: A Review. *Energy* **2023**, *16*, 2960. [[CrossRef](#)]
44. Shi, Z.; Li, M.; Liang, H.; Zhou, K.; Gong, X.; Lin, J. Understanding Safety Risk Warning Technologies for Lithium-Ion Battery Energy Storage Power Stations from an Engineering Perspective. In Proceedings of the 2025 2nd International Conference on Smart Grid and Artificial Intelligence (SGAI), Changsha, China, 21–23 March 2025; pp. 1052–1055. [[CrossRef](#)]
45. Deng, Q. Development Status of Safety Technologies of Lithium-ion Battery Energy Storage System. *Sino-Glob. Energy* **2022**, *27*, 93–99. [[CrossRef](#)]
46. Liu, J.; Lei, H.; Lv, J.; Wang, Y.; Xu, D. SOC Estimation of Lithium-ion Batteries Based on CNN-LSTM. *Electr. Drive* **2024**, *54*, 26–31. [[CrossRef](#)]
47. Wu, H.; Huang, X.; Qiao, Z.; Fan, Y.; Zhu, J.; Chen, J. SOH Estimation of Lithium-ion Batteries Based on Multiple Feature Combinations. *Electr. Drive* **2025**, *55*, 25–32, 40. [[CrossRef](#)]
48. Fan, Y.; Zhu, J.; Wu, H.; Han, X.; Huang, X.; Chen, J. State of Health Estimation Method for Lithium-ion Batteries in Energy Storage Systems Based on Two-stage Charging Data. *Electr. Drive* **2025**, *55*, 72–80. [[CrossRef](#)]
49. Zheng, K.; Meng, J.; Yang, Z.; Zhou, F.; Yang, K.; Song, Z. Refined Lithium-Ion Battery State of Health Estimation with Charging Segment Adjustment. *Appl. Energy* **2024**, *375*, 124077. [[CrossRef](#)]
50. Sun, L.; Sun, W.; You, F. Core Temperature Modelling and Monitoring of Lithium-Ion Battery in the Presence of Sensor Bias. *Appl. Energy* **2020**, *271*, 115243. [[CrossRef](#)]
51. Mei, W.; Liu, Z.; Wang, C.; Wu, C.; Liu, Y.; Liu, P.; Xia, X.; Xue, X.; Han, X.; Sun, J.; et al. Operando monitoring of thermal runaway in commercial lithium-ion cells via advanced lab-on-fiber technologies. *Nat. Commun.* **2023**, *14*, 5251. [[CrossRef](#)] [[PubMed](#)]
52. Fernandes, Y.; Bry, A.; de Persis, S. Identification and Quantification of Gases Emitted during Abuse Tests by Overcharge of a Commercial Li-Ion Battery. *J. Power Sources* **2018**, *389*, 106–119. [[CrossRef](#)]
53. Leng, X.; Li, Y.; Xu, G.; Xiong, W.; Xiao, S.; Li, C.; Chen, J.; Yang, M.; Li, S.; Chen, Y.; et al. Prediction of lithium-ion battery internal temperature using the imaginary part of electrochemical impedance spectroscopy. *Int. J. Heat Mass Transf.* **2025**, *240*, 126664. [[CrossRef](#)]
54. Lei, J.; Li, Z.; Chen, B.; Huang, D. Estimation of internal battery temperature based on electrochemical impedance spectroscopy. *Energy Storage Sci. Technol.* **2024**, *13*, 2823. [[CrossRef](#)]
55. Kim, J.; Kim, E.; Lee, U.; Lee, I.; Han, S.; Son, H.; Yoon, S. Nondisruptive In Situ Raman Analysis for Gas Evolution in Commercial Supercapacitor Cells. *Electrochim. Acta* **2016**, *219*, 447–452. [[CrossRef](#)]

56. Jin, Y.; Zheng, Z.; Wei, D.; Jiang, X.; Lu, H.; Sun, L.; Tao, F.; Guo, D.; Liu, Y.; Guo, J.; et al. Detection of Micro-Scale Li Dendrite via H₂ Gas Capture for Early Safety Warning. *Joule* **2020**, *4*, 1714–1729. [CrossRef]
57. Zheng, Z. Study on Thermal Runaway and Safety Warning via GasDetection of LiFePO₄ Energy Storage Battery under Overcharge Condition. Master’s Thesis, Zhengzhou University, Zhengzhou, China, 2022.
58. Wang, M.; Sun, L.; Guo, P.; Guo, D.; Zhao, L.; Jin, Y. Overcharge and Thermal Runaway Characteristics of Lithium Iron Phosphate Energy Storage Battery Modules Based on Gas Online Monitoring. *High Volt. Eng.* **2021**, *47*, 279–286. [CrossRef]
59. Zhang, J.; Ma, C.; Liu, S.; Guo, Q.; Liu, S.; Han, P.; Huang, Z.; Han, D. Chemical Reaction Neural Networks to Map Lithium-Ion Battery Thermal Runaway Gas Generation. *Cell Rep. Phys. Sci.* **2025**, *6*, 102563. [CrossRef]
60. Lu, L.; Han, X.; Li, J.; Hua, J.; Ouyang, M. A Review on the Key Issues for Lithium-Ion Battery Management in Electric Vehicles. *J. Power Sources* **2013**, *226*, 272–288. [CrossRef]
61. Wang, Q.; Ping, P.; Zhao, X.; Chu, G.; Sun, J.; Chen, C. Thermal Runaway Caused Fire and Explosion of Lithium Ion Battery. *J. Power Sources* **2012**, *208*, 210–224. [CrossRef]
62. Chouchane, M.; Rucci, A.; Lombardo, T.; Ngandjong, A.C.; Franco, A.A. Lithium Ion Battery Electrodes Predicted from Manufacturing Simulations: Assessing the Impact of the Carbon-Binder Spatial Location on the Electrochemical Performance. *J. Power Sources* **2019**, *444*, 227285. [CrossRef]
63. Wei, Z.; Zhong, G.; Su, W.; Wang, W.; Zhang, Y.; Liu, K.; Liu, H. Float-Charging Characteristics of Lithium Iron Phosphate Battery Based on Direct-Current Power Supply System in Substation. *J. Energy Eng.* **2016**, *142*, 04015016. [CrossRef]
64. Bi, H.; Zhu, H.; Zu, L.; Gao, Y.; Gao, S.; Peng, J.; Li, H. Low-Temperature Thermal Pretreatment Process for Recycling Inner Core of Spent Lithium Iron Phosphate Batteries. *Waste Manag. Res.* **2020**, *39*, 146–155. [CrossRef]
65. Fang, Z.; Junming, L.; Xiaochen, Y.; Hainan, S.; Xin, Y.; Jing, P.; Hongxu, X. Safety Analysis and System Design of Lithium Iron Phosphate Battery in Substation. *E3S Web Conf.* **2021**, *256*, 01017. [CrossRef]
66. Li, J.; Qu, S.; Ma, s.; Zeng, W.; Xiong, J. Research On Frequency Modulation Control Strategy Of Auxiliary Power Grid In Battery Energy Storage System. *Acta Energiae Solaris Sin.* **2023**, *44*, 326–335. [CrossRef]
67. Jin, Y.; Su, T.; Jiang, X.; Gao, J.; Lv, N. Silicon–Carbon Composite Anode Material for Lithium-Ion Batteries and Its Preparation Method. Chinese Patent CN201910529522.3, 30 August 2019.
68. Li, R.; Guo, F.; Zhao, G. Early Warning Method for Fire Safety of Containerized Lithium-Ion Battery Energy Storage Systems. *Energy Storage Sci. Technol.* **2024**, *13*, 1595. [CrossRef]
69. Su, T. Research on Safety Warning and Fault Location of Lithium Battery Energy Storage Cabin Based on Acoustic Signal. Master’s Thesis, Zhengzhou University, Zhengzhou, China, 2021. [CrossRef]
70. Xie, L.; Wang, L.; Zhou, H.; Weng, D.; Yang, P.; Zhong, L. Early Warning System of Lithium Battery Running State Based on Neural Network and Voiceprint Recognition. *Integr. Circuits Embed. Syst.* **2023**, *23*, 45–49.
71. Shen, Y.; Wang, X.; Li, Y.; Zhang, Z.; Tao, Z.; Hou, Y.; Wei, X.; Dai, H. Expansion Force-Based Adaptive Multistage Constant Current Fast Charging with Lithium Plating Detection for Lithium-Ion Batteries. *Adv. Sci.* **2025**; early view. [CrossRef]
72. Li, K.; Li, J.; Gao, X.; Lu, Y.; Wang, D.; Zhang, W.; Wu, W.; Han, X.; Cao, Y.; Lu, L.; et al. Effect of Preload Forces on Multidimensional Signal Dynamic Behaviours for Battery Early Safety Warning. *J. Energy Chem.* **2024**, *92*, 484–498. [CrossRef]
73. Figueroa-Santos, M.A.; Siegel, J.B.; Stefanopoulou, A.G. Leveraging Cell Expansion Sensing in State of Charge Estimation: Practical Considerations. *Energies* **2020**, *13*, 2653. [CrossRef]
74. Cai, T.; Pannala, S.; Stefanopoulou, A.G.; Siegel, J.B. Battery Internal Short Detection Methodology Using Cell Swelling Measurements. In Proceedings of the 2020 American Control Conference (ACC), Denver, CO, USA, 1–3 July 2020; pp. 1143–1148. [CrossRef]
75. Aufschläger, A.; Kücher, S.; Kraft, L.; Spingler, F.; Niehoff, P.; Jossen, A. High Precision Measurement of Reversible Swelling and Electrochemical Performance of Flexibly Compressed 5Ah NMC622/Graphite Lithium-Ion Pouch Cells. *J. Energy Storage* **2023**, *59*, 106483. [CrossRef]
76. Hemmerling, J.; Schäfer, J.; Jung, T.; Kreher, T.; Ströbel, M.; Gassmann, C.; Günther, J.; Fill, A.; Birke, K.P. Investigation of Internal Gas Pressure and Internal Temperature of Cylindrical Li-Ion Cells to Study Thermodynamical and Mechanical Properties of Hard Case Battery Cells. *J. Energy Storage* **2023**, *59*, 106444. [CrossRef]
77. Chang, Y.; Cheng, Y.; Jia, R.; Wang, R.; Xu, Q.; Gong, L.; Wei, Y.; Tang, B.; Guo, C.; Sun, B.; et al. Unified Iontronic Sensing for Operando Monitoring of Physical-Chemical Events in Lithium-Ion Batteries. *Natl. Sci. Rev.* **2025**, *12*, nwaf151. [CrossRef]
78. Zhao, Y.; Spingler, F.B.; Patel, Y.; Offer, G.J.; Jossen, A. Localized Swelling Inhomogeneity Detection in Lithium Ion Cells Using Multi-Dimensional Laser Scanning. *J. Electrochem. Soc.* **2019**, *166*, A27. [CrossRef]
79. Yu, X.; Feng, Z.; Ren, Y.; Henn, D.; Wu, Z.; An, K.; Wu, B.; Fau, C.; Li, C.; Harris, S.J. Simultaneous Operando Measurements of the Local Temperature, State of Charge, and Strain inside a Commercial Lithium-Ion Battery Pouch Cell. *J. Electrochem. Soc.* **2018**, *165*, A1578. [CrossRef]
80. Ozdogru, B.; Padwal, S.; Bal, B.; Harimkar, S.; Koohbor, B.; Çapraz, Ö.Ö. Coupling between Voltage Profiles and Mechanical Deformations in LAGP Solid Electrolyte During Li Plating and Stripping. *ACS Appl. Energy Mater.* **2022**, *5*, 2655–2662. [CrossRef]

81. Wang, L.; Liu, G.; Deng, Y.; Sun, W.; Ma, Q.; Ma, S. Investigation on Out-of-Plane Displacement Measurements of Thin Films via a Mechanical Constraint-Based 3D-DIC Technique. *Opt. Commun.* **2023**, *530*, 129015. [[CrossRef](#)]
82. Tang, W.; Jiang, X.; Liu, H.; Jin, Y. Early Warning of Lithium-ion Battery Fire Based on Image Recognition of Gas-liquid Escape. *High Volt. Eng.* **2022**, *48*, 3295–3304. [[CrossRef](#)]
83. Shi, Z.; Zhou, Y.; Cheng, X. Smoke scattering characteristics of electrolyte fire of lithium-ion battery. *Fire Saf. Sci.* **2021**, *30*, 107–112. [[CrossRef](#)]
84. Lin, G. Research on early fire detection technology of lithium-ion battery storage area based on AI technology. *Fire Sci. Technol.* **2022**, *41*, 686–689, 693. [[CrossRef](#)]
85. Shi, B.; Li, M.; Ye, J. Analysis on application status of thermal management technology for lithium ion battery energy storage. *Chin. J. Power Sources* **2023**, *47*, 562–569.
86. Liu, S.; Li, H.; Zhang, J.; Zeng, G.; Xu, L. A study on the synergistic optimization of flow channel structures and guide plates in a 280 Ah air-cooled battery pack for energy storage. *Energy Storage Sci. Technol.* **2025**, *14*, 1806–1817. [[CrossRef](#)]
87. Chen, K.; Wu, W.; Yuan, F.; Chen, L.; Wang, S. Cooling Efficiency Improvement of Air-Cooled Battery Thermal Management System through Designing the Flow Pattern. *Energy* **2019**, *167*, 781–790. [[CrossRef](#)]
88. Xie, J.; Ge, Z.; Zang, M.; Wang, S. Structural Optimization of Lithium-Ion Battery Pack with Forced Air Cooling System. *Appl. Therm. Eng.* **2017**, *126*, 583–593. [[CrossRef](#)]
89. Yu, K.; Yang, X.; Cheng, Y.; Li, C. Thermal Analysis and Two-Directional Air Flow Thermal Management for Lithium-Ion Battery Pack. *J. Power Sources* **2014**, *270*, 193–200. [[CrossRef](#)]
90. Sun, R.; Guo, D.; Zhang, Z.; Xiao, P.; Sun, L. Optimization and Verification of Thermal Characteristics of LiFePO₄ Battery Energy Storage Module with Parallel Serpentine Flow Channel Structure. *J. Power Supply*, **2025**; *early access*.
91. Zhang, Y.; Zuo, W.; Li, J.; Li, Q.; Sun, K.; Zhou, K.; Zhang, G. Performance Comparison between Straight Channel Cold Plate and Inclined Channel Cold Plate for Thermal Management of a Prismatic LiFePO₄ Battery. *Energy* **2022**, *248*, 123637. [[CrossRef](#)]
92. Yao, G.; You, X.; Zhou, L.; Luo, C.; Yu, T.; Wang, J. Optimization design of PCS liquid cooled radiator based on multi-objective gray wolf optimizer. *Adv. Technol. Electr. Eng. Energy* **2025**, *44*, 1–11. [[CrossRef](#)]
93. Zeng, S.; Wu, W.; Liu, J.; Wang, S.; Ye, S.; Feng, Z. A review of research on immersion cooling technology for lithium-ion batteries. *Energy Storage Sci. Technol.* **2023**, *12*, 2888. [[CrossRef](#)]
94. Ji, P.; Guo, L.; Tao, H. Summarize of effect of thermal management strategy on the performance of battery energy storage system. *Battery Bimon.* **2025**, *55*, 178–185. [[CrossRef](#)]
95. Yuan, J.; Wang, L.; Tan, Y.; Jiao, Y. Experimental Study on Refrigeration System of Phase-change Energy Storage for High-power Applications. *J. Refrig.* **2020**, *41*, 124–130.
96. Mills, A.; Al-Hallaj, S. Simulation of Passive Thermal Management System for Lithium-Ion Battery Packs. *J. Power Sources* **2005**, *141*, 307–315. [[CrossRef](#)]
97. Li, Y.; Yuan, X.; Yang, Z. Construction and thermal characteristics of foam aluminum-polyethylene glycol phase change energy storage materials. *New Chem. Mater.* **2025**; *early access*.
98. Zheng, L.; Zhi, M.; Yue, S.; Pan, Z. Hydrated salt phase change composite used in thermal management of Li-ion battery. *Battery Bimon.* **2024**, *54*, 217–221. [[CrossRef](#)]
99. Zhong, G.; Wang, Y.; Wang, C.; Wang, J.; Su, W.; Chen, J. The review of thermal management technology for large-scale lithium-ion battery energy storage system. *Energy Storage Sci. Technol.* **2018**, *7*, 203–210.
100. Feng, J.; Wu, W. Research progress on liquid cooling thermal management technology for energy storage. *Refrig. Air Cond.* **2024**, *24*, 1–11, 16. [[CrossRef](#)]
101. Jaidi, J.; Chitta, S.D.; Akkaldevi, C.; Panchal, S.; Fowler, M.; Fraser, R. Performance Study on the Effect of Coolant Inlet Conditions for a 20 Ah LiFePO₄ Prismatic Battery with Commercial Mini Channel Cold Plates. *Electrochim.* **2022**, *3*, 259–275. [[CrossRef](#)]
102. Chang, Q.; Huang, Y.; Liu, K.; Xu, X.; Zhao, Y.; Pan, S. Optimization Control Strategies and Evaluation Metrics of Cooling Systems in Data Centers: A Review. *Sustainability* **2024**, *16*, 7222. [[CrossRef](#)]
103. Chen, D.; Jiang, J.; Kim, G.; Yang, C.; Pesaran, A. Comparison of different cooling methods for lithium ion battery cells. *Appl. Therm. Eng.* **2016**, *94*, 846–854. [[CrossRef](#)]
104. Yuan, S.; Chang, C.; Yan, S.; Zhou, P.; Qian, X.; Yuan, M.; Liu, K. A Review of Fire-Extinguishing Agent on Suppressing Lithium-Ion Batteries Fire. *J. Energy Chem.* **2021**, *62*, 262–280. [[CrossRef](#)]
105. Liu, H.; Wang, S.; Bai, B. Comparative study on the key performance of waterbased types extinguishing agent for liquid fire. *Fire Sci. Technol.* **2024**, *43*, 1424–1428. [[CrossRef](#)]
106. Ji, C.; Liu, Y.; Qi, P.; Zhang, Z.; Zhang, S. Simulation Investigation of Water Spray on Suppressing Lithium-Ion Battery Fires. *Fire Technol.* **2023**, *59*, 1221–1246. [[CrossRef](#)]
107. Zhang, Y.; Peng, W.; Liu, X. Study on retarding effect of water mist containing additive on thermal runaway of lithium battery. *Fire Sci. Technol.* **2024**, *43*, 504–509, 577. [[CrossRef](#)]

108. Kumar, M.; Barbhui, M. Sustainable fire safety solutions: Bioactive natural polysaccharides and secondary metabolites as innovative fire retardants for textiles. *Emerg. Manag. Sci. Technol.* **2023**, *3*, 17. [[CrossRef](#)]
109. Hynes, R.G.; Mackie, J.C.; Masri, A.R. Sample Probe Measurements on a Hydrogen–Ethane–Air–2-H-Heptafluoropropane Flame. *Energy Fuels* **1999**, *13*, 485–492. [[CrossRef](#)]
110. Yu, D.; Li, Y.; Zhang, S.; Du, Y. Study on efficiency of HFC-227 for extinguishing Li-ion power battery fire. *Chin. J. Power Sources* **2019**, *43*, 60–63. [[CrossRef](#)]
111. Xie, Z.; Wang, Z.; Zhang, G.; Gu, Z.; Yao, B. Experimental study on fire extinguishing of large-capacity ternary lithium-ion battery by perfluorohexanone and water mist fire extinguishing device. *Energy Storage Sci. Technol.* **2022**, *11*, 652–659. [[CrossRef](#)]
112. Wang, Q.; Shao, G.; Duan, Q.; Chen, M.; Li, Y.; Wu, K.; Liu, B.; Peng, P.; Sun, J. The Efficiency of Heptafluoropropane Fire Extinguishing Agent on Suppressing the Lithium Titanate Battery Fire. *Fire Technol.* **2016**, *52*, 387–396. [[CrossRef](#)]
113. Jia, Z.; Jin, K.; Mei, W.; Qin, P.; Sun, J.; Wang, Q. Advances and Perspectives in Fire Safety of Lithium-Ion Battery Energy Storage Systems. *eTransportation* **2025**, *24*, 100390. [[CrossRef](#)]
114. Bai, Z.; Li, X.; Deng, J.; Shu, C.-M.; Zhang, Y.; Zhang, P.; Ramakrishna, S. Overview of Anti-Fire Technology for Suppressing Thermal Runaway of Lithium Battery: Material, Performance, and Applications. *J. Power Sources* **2025**, *640*, 236767. [[CrossRef](#)]
115. Zhang, L.; Li, Y.; Duan, Q.; Chen, M.; Xu, J.; Zhao, C.; Sun, J.; Wang, Q. Experimental Study on the Synergistic Effect of Gas Extinguishing Agents and Water Mist on Suppressing Lithium-Ion Battery Fires. *J. Energy Storage* **2020**, *32*, 101801. [[CrossRef](#)]
116. Lu, J.; Zhou, T.; Wu, C. Study on Fire Extinguishing and Anti-Reburning Technology of Lithium-Ion Battery Energy Storage System. *Hunan Electr. Power* **2022**, *42*, 6+14. [[CrossRef](#)]
117. Zhang, L.; Duan, Q.; Meng, X.; Jin, K.; Xu, J.; Sun, J.; Wang, Q. Experimental Investigation on Intermittent Spray Cooling and Toxic Hazards of Lithium-Ion Battery Thermal Runaway. *Energy Convers. Manag.* **2022**, *252*, 115091. [[CrossRef](#)]
118. Meng, X.; Li, S.; Fu, W.; Chen, Y.; Duan, Q.; Wang, Q. Experimental Study of Intermittent Spray Cooling on Suppression for Lithium Iron Phosphate Battery Fires. *eTransportation* **2022**, *11*, 100142. [[CrossRef](#)]
119. Lou, P.; Zhang, W.; Han, Q.; Tang, S.; Tian, J.; Li, Y.; Wu, H.; Zhong, Y.; Cao, Y.-C.; Cheng, S. Fabrication of Fire-Response Functional Separators with Microcapsule Fire Extinguishing Agent for Lithium-Ion Battery Safety. *Nano Sel.* **2022**, *3*, 947–955. [[CrossRef](#)]
120. Zheng, G.; Yang, Z.; Gao, C. A Safety Warning Method and Device for Lithium-Ion Batteries. Chinese Patent CN109453491A, 12 March 2019.
121. Yang, B. Research on Microencapsulation Technology of Perfluorohexanone Fire Extinguishing Agent. Master’s Thesis, Nanjing University of Science and Technology, Nanjing, China, 2021. [[CrossRef](#)]
122. Liu, Y.; Duan, Q.; Xu, J.; Li, H.; Sun, J.; Wang, Q. Experimental Study on a Novel Safety Strategy of Lithium-Ion Battery Integrating Fire Suppression and Rapid Cooling. *J. Energy Storage* **2020**, *28*, 101185. [[CrossRef](#)]
123. Wang, J.; Yu, K.; Xiao, P.; Li, L.; Wang, C.; Wang, Z.; Guo, D.; Yuen Kwok, K.; Lu, Y. Killing two birds with one stone strategy inspired advanced batteries with superior thermal safety: A comprehensive evaluation. *Chem. Eng. J.* **2025**, *515*, 163272. [[CrossRef](#)]

Disclaimer/Publisher’s Note: The statements, opinions and data contained in all publications are solely those of the individual author(s) and contributor(s) and not of MDPI and/or the editor(s). MDPI and/or the editor(s) disclaim responsibility for any injury to people or property resulting from any ideas, methods, instructions or products referred to in the content.